Application of Non Local Means Filter and Sparse Spike Deconvolution for Seismic Processing. Reappraisal of Rotliegend and Dinantian formations in the Netherlands.

by

Muhammad Hanif Abidin

A THESIS

submitted to

Utrecht University

in partial fulfillment of
the requirements for the
degree of

Master of Science

Presented 2018
Commencement July 2018

TABLE OF CONTENTS

LIST OF FIGURES

Figure Page

LIST OF FIGURES (Continued)

Figure Page

LIST OF FIGURES (Continued)

Figure Page

Abstract

Conventional seismic reprocessing and new unconventional methods, the Non Local Means algorithm and Sparse Spiked Deconvolution are applied to a real 2D Seismic Dataset. The aim is to get better images on the Rotliegend and Dinantian formations which are the target of Geothermal Exploration in the Netherlands. Conventional seismic reprocessing gives improvement over the seismic data, particularly due to the superior Pre-Stack Kirchhoff Time Migration used. Non Local Means Algorithm proven to increase signal to noise ratio of the seismic data while preserving fault edges. We propose different NLM workflow with different parameters for different processing target. Sparse Spike deconvolution with combined ℓ_1 norm and ℓ_2 norm regularization for maximum sparsity and smoothness constraints is found to increase vertical resolution and preserves reflection amplitudes and structures, reveals new reflection packages and small geological features emerge from the data. Although NLM and Sparse Spike deconvolution are found to improve the signal to noise ratio and vertical resolution in the mid depth section of Rotliegend reservoir, the offset limitation factor still hampers the imaging of deep section of Dinantian reservoir. We suggest for new seismic acquisition to use larger offset to get the maximum results on the Dinantian reservoir imaging

1 Introduction

The geothermal potential of ultra-deep reservoir formations in the Netherlands has been investigated in the recent years as a result of push for development of sustainable and unconventional energy resources in Europe, with in The Netherlands particular interest in ultra-deep lower Carboniferous Dinantian carbonate reservoir systems. As one of the major hydrocarbon provinces in western Europe, The Netherlands has good seismic coverage on-shore and off-shore as well as more than 5000 oil and gas wells. There has been much detailed study of the first two to three kilometers of the Dutch subsurface (T. E. Wong, Batjes, and Jager 2007), however only few studies were done below the Permian Upper Rotliegend (Van Hulten 2012).

Dinantian age formations in the Netherlands are generally found below 3500 m, and they are rarely considered a hydrocarbon exploration target. Figure 1.1 shows the interpreted top of Dinantian in seismic two way time (ms). There are only few wells drilled penetrating the Dinantian, and seismic imaging did not have a focus on deep reservoirs due to the strong emphasis on shallower Permian Rotliegend gas play. It was common practice to cut off the lower parts of commercial seismic line because of very low signal to noise ratio (Van Hulten 2012).

Also for more conventional depths (∼2000 m) the development of the geothermal sector in the province of Utrecht is hampered by the poor quality of seismic data. The little available seismic data allows mapping of the top of the Rotliegend reservoir, however is of too low quality to map its thickness. The thickness uncertainty (which scales linearly to geothermal power) may be in the order of up to 50%(TNO). Based on this fact, it is important to get seismic sections with better quality for geothermal exploration in the Netherlands targeting Rotliegend and deep Dinantian formations.

1.1 Seismic Reflection Challenges for Geothermal Prospecting

Seismic reflection imaging is the geophysical method with the highest accuracy for acquiring subsurface information at great depth, therefore it has been used extensively for oil and gas exploration. For geothermal exploration, it has only been sparingly used due to some limitations. In the magmatic environment for example, active seismic surveying is not suitable due to terrain acquisition difficulties and strong signal attenuation due to volcanic rocks and magma chambers. In this environment, passive seismic method is more commonly used.

In the enhanced geothermal setting such as in the Netherlands, seismic reflection imaging does not have such problems, although it has other challenges. Ultra deep Enhanced geothermal systems (EGS) need ultra-high depth (greater than ∼3000 m) to reach sufficient temperatures, and are usually are located in the crystalline basement rock or carbonates with low permeability. The key challenges of seismic reflection imaging in this type of environment are (1) weak reflection amplitudes which leads to low signal to noise ratio, (2) complex morphology, lithology, and deformation which leads to often small, steeply dipping, and laterally discontinuous reflectors, (3) resolution loss in the crystalline basement due to relatively longer wavelength, (4) offset limitation to acquire proper migration and velocity models in the deeper structures, and (5) fractures and layering leading to complex wave propagation and anisotropy (Schmelzbach et al. 2016). Milkrereit and

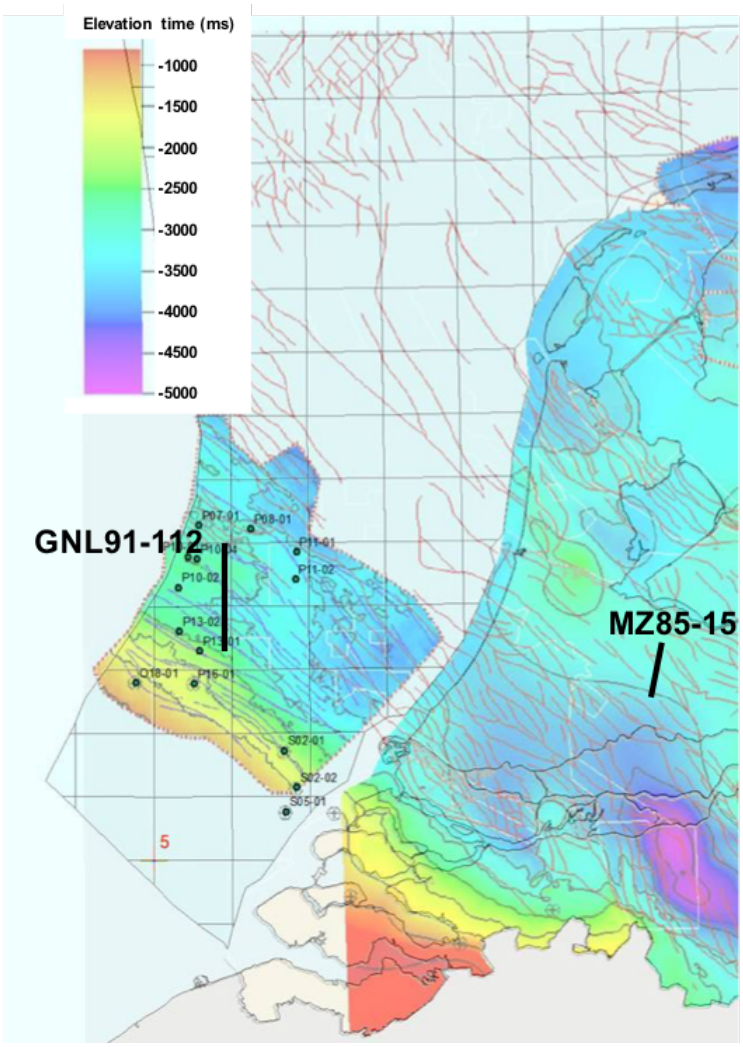

Figure 1.1: Depth in two way time (ms) map of top of the Dinantian in the Netherlands (Jaarsma et al. 2013). Location of Marine Line GNL19-112 and Land Line MZ85-18 used in this research are shown.

Eaton (Milkereit and Eaton 1998) discuss in detail the challenges of seismic imaging in crystalline basement compared to sedimentary basins.

In this research, conventional seismic reprocessing of the pre-stack data combined with new unconventional processing techniques are done to improve the seismic image of an off-shore line and an on-shore line in the Netherlands. The unconventional processing techniques used are the Non Local Means Filter (Buades, Coll, and Morel 2005) and Seismic Sparse Spike Deconvolution (Chapman and Barrodale 1983). The Non-Local Means filter aims to enhance the signal to noise ratio, especially in the deep Dinantian reflector where low signal to noise ratio has been the major problem of depth interpretation. The major advantage of Non-Local Means filtering over the commonly used coherency filtering such as FX Deconvolution (Galbraith et al. 1991) is that NLM has strong edge preservation properties which is important in enhanced geothermal system where faults and fractures are important features needed to be preserved. Sparse spike deconvolution using ℓ_1 norm regularization aims to increase the vertical resolution of the seismic image and thus enhance

the limited seismic bandwidth, which will improve the accuracy of seismic interpretation for geothermal exploration.

The conventional seismic pre-processing itself is expected to bring significant improvement over the old seismic data due to technological advancement in the seismic processing algorithm throughout the years. The additional unconventional techniques are expected to bring more improvements to get better image of the subsurface, especially Rotliegend and Dinantian structures.

By enhancing the overall quality of seismic sections using conventional reprocessing, non-local means filter, and seismic bandwidth enhancement, a better depth model of Rotliegend and Dinantian formation in the Netherlands can be obtained, thus reducing uncertainties in the key geothermal reservoir parameters which are important in successful geothermal exploration.The conventional and new techniques mentioned above and their application will be investigated, to see how far they improve the quality of Rotliegend and deep Dinantian formations.

2 Methodology

The Methodology used in this research is the application of Non Local Means Algorithm and Sparse spike deconvolution following a seismic reprocessing of real 2D seismic datasets. In this research seismic processing of seismic data are done using conventional methods commonly used in the industry (Yilmaz 2001). The datasets used are a 2D offshore (GNL19-112) line located north of the Zeeland province of the Netherlands and a 2D onshore line (HZ85-15) located south of Utrecht University campus of De Uithof, the Netherlands (Figure 2.1). The datasets have been processed before in 1980s and both pre-stack and post-stack seismic data are publicly available (nlog.nl). The MZ81-15 land line in the Utrecht area is located on one of the focus areas for Rotliegend & Dinantian exploration in the Netherlands. The GNL91-112 line was chosen to show the effectiveness of the method to resolve deep structures in marine seismic, as the Dinantian reflectors in this area are located quite deep, around 3000 ms (Figure 1.1).

The conventional seismic processing up to Migration are done in Globe Claritas and Non Local means filter and Sparse spike deconvolution are done in Matlab. The results and method are evaluated by seismic-well tie using Schlumberger Petrel and the previous interpreted depth model of Dinantian and Rotliegend Netherlands formation (TNO).

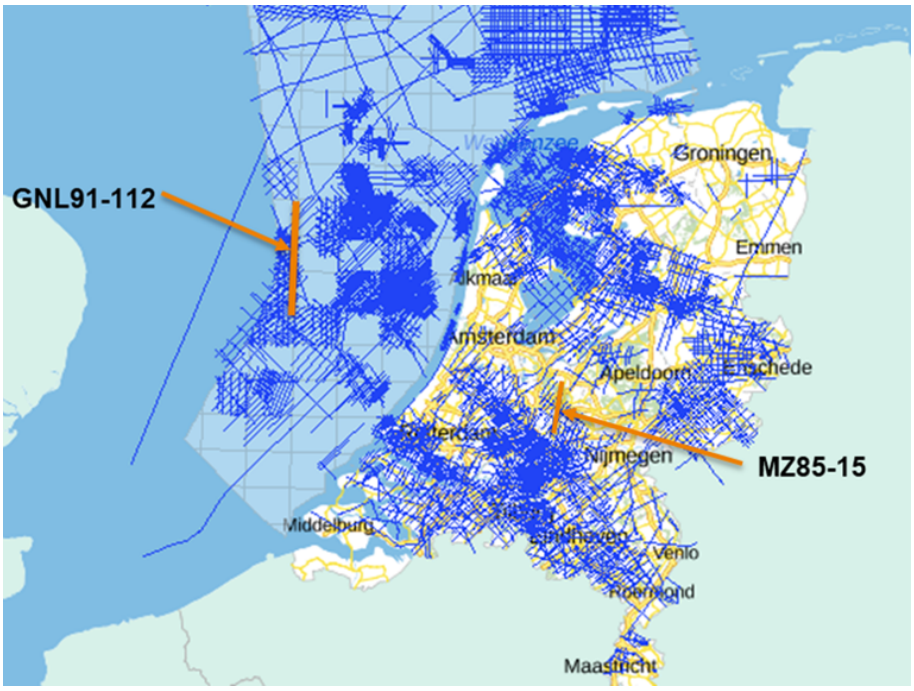

Figure 2.1: Map showing location of Marine Line GNL19-112 and Land Line MZ85-18 used in this research. Source : http://nlog.nl

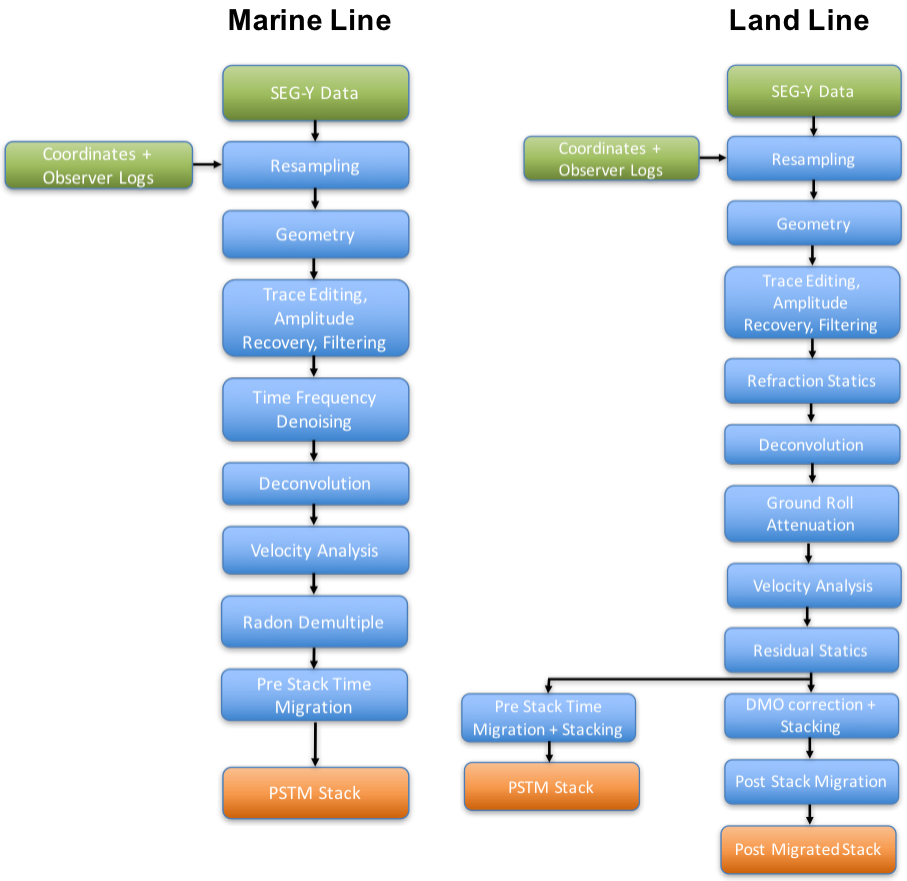

Figure 2.2: Seismic processing workflow using conventional method (Yilmaz) of the marine data (left) and land data (right). Post Stack Time Migration and Pre Stack Time Migration are done on the land data due to poor imaging of deep section of PSTM. Limited offset and short line length induces strong artifacts of the deep section. From shallow to mid depth section PSTM results are superior on both marine and land lines.

2.1 Seismic Processing

The pre-stack seismic processing is done using conventional workflow (Yilmaz 2001) commonly used in the oil and gas industry. The goal of seismic processing is to get the most accurate image of the earth subsurface from the recorded field seismic data. By doing seismic processing, we compensate for the acquisition effects, increase the signal to noise ratio, minimize the signal distortion, and concentrate the recorded wave field data. Marine seismic data and land seismic data have different characteristics and needs different processing strategy. Marine seismic data typically has a more regular geometry, higher folds, and stronger coherent noise (Yilmaz 2001). Common coherent noises found in marine data are swell noise, which is the results of hydrostatic pressure changes in the seismic streamer and multiples. Multiple is a recorded wave which has undergone more than one reflection in its travel path, and its attenuation is one of the major challenges in marine seismic data processing. In land data, the main characteristics are irregular geometry and elevation, low signal to noise ratio, strong incoherent (random) noise, and the presence of strong ground roll noise (surface waves). Due to irregular terrain and the presence of low velocity layer near the surface in land data acquisition, statics corrections are needed.

Figure 2.2 shows the full workflow of the conventional processing for the offshore and onshore line. In the case of marine line (GNL9-112) the radon demultiple step to eliminate multiple reflections is applied before migration, and for the onshore line (HZ85-15) refraction and residual statics and ground roll attenuations are done. The final product of conventional processing workflow is a time migrated seismic section which is an approximation of the real subsurface structures in two-way time domain. Hence the result can be directly compared to the old processed post-stack migrated sections. The most important steps which affects the reprocessing result, will be explained in detail in this chapter, while the other routines and results comparison of the conventional processing can be found in Appendix 1

2.1.1 Preprocessing

Preprocessing is the earliest step in seismic processing after SEG-Y file input. This starts by resampling the input data to 4ms (based on the previous processing report and frequency content of the data) and then merging geometry information with the data. Geometry application assigns source and receiver coordinates into the trace headers as well as source receiver relations or spread information. This allows us to make CDP and offset calculation for stacking and other processing steps. Geometry is one of the most important step of processing, as many problems in processing arise due to incorrect geometry (Yilmaz 2001). For the land data, elevation statics are also applied. One of the important steps in preprocessing is gain correction to recover the amplitude loss by spherical wave front divergence.

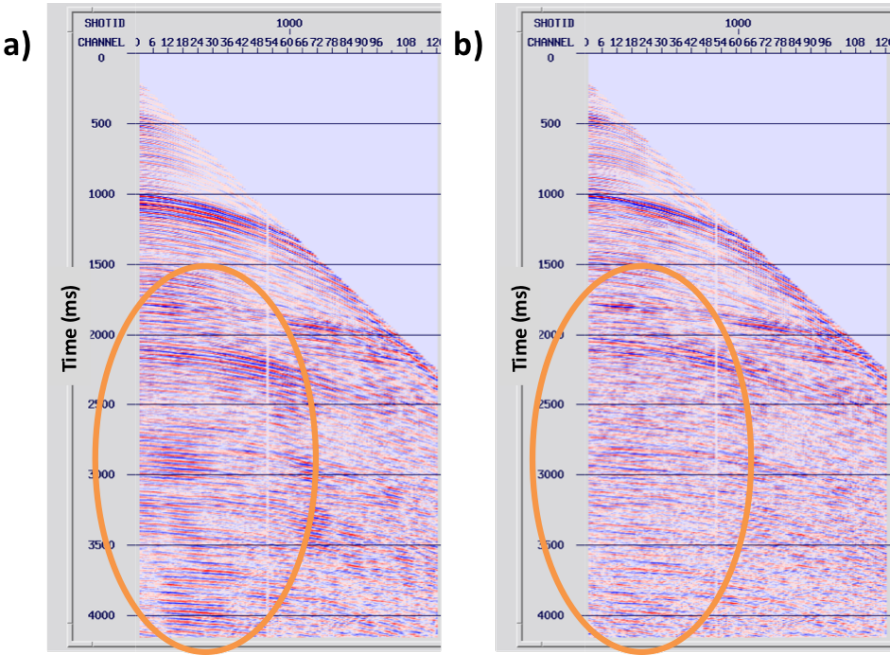

Figure 2.3: a) Before and b) after deconvolution using operator length 150 ms and gap length 16 ms on the marine line GNL19-112 shot gather. The orange circles shows reverberations and short period multiples are attenuated after deconvolution.

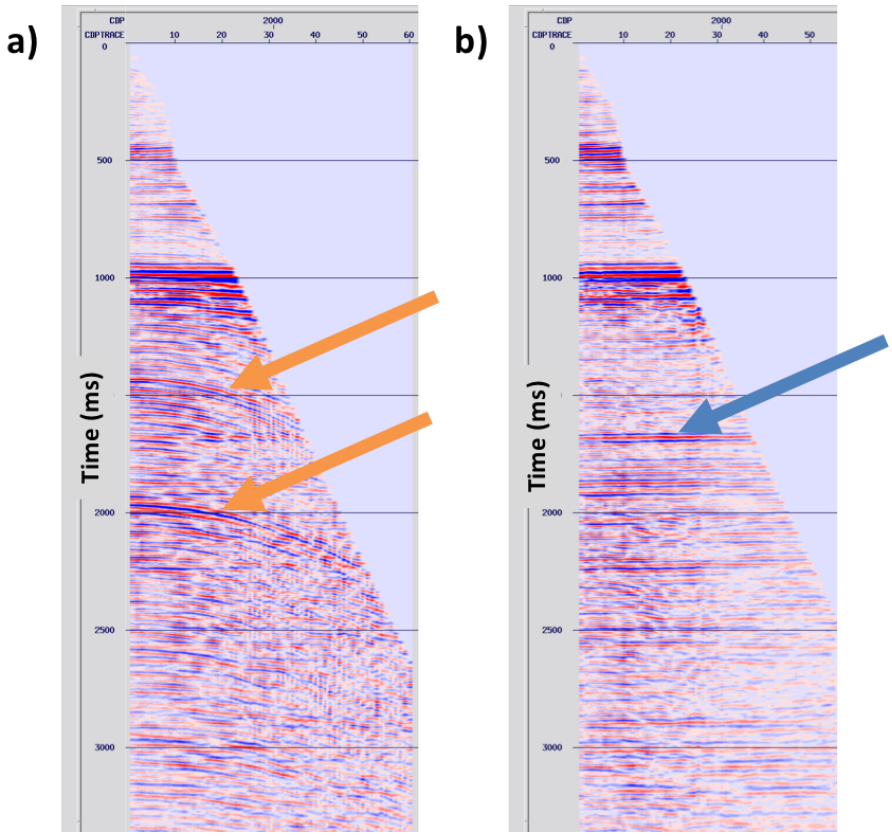

Figure 2.4: a) Before and b) after Radon demultiple on the marine line GNL19-112 cdp gather. The orange arrow shows suppressed long period multiple and blue arrow shows enhanced primary reflector after demultiple

2.1.2 Statics Correction

There are two statics correction method which are usually applied in land seismic processing, refraction statics and residual statics. Refraction statics require the near surface model knowledge which consist of a low velocity weathering layer, although in other cases such as glacial tills and sand dunes it may consist of more than one low velocity layer (Yilmaz 2001). The first arrivals on the shot gather can be assumed as the refracted energy from the base of the weathering layer. Hence to do refraction statics we need these first arrivals information, which is acquired by a processing step known as first break picking. In this research first break picking is done automatically using Globe Claritas automatic picking tools and few manual corrections. For large 3D land datasets, a superior auto picking algorithm will really help as first break picking is one of the most time consuming steps. This is especially true for data with poor quality and has lots of first arrivals uncertainties.

2.1.3 Deconvolution

Deconvolution aims to increase the temporal resolution and compresses the wavelet. It also attenuates reverberations and short period multiples, which is our main objective in this step. The deconvolution in the conventional workflow differs to the later unconventional sparse spike deconvolution method using ℓ_1

norm regularization. The deconvolution here is Wiener deconvolution in which it uses the commonly used $l\ell_2$ norm regularization or least squares inversion method which is less computationally demanding. The details about the deconvolution process will be explained in the section about Sparse Spike deconvolution. The predictive Wiener deconvolution used in this step requires the selection of appropriate operator and gap lengths to get the desired wavelet and to prevent artifacts. In the land data MZ85-15, deconvolution introduces low frequency noise which is a common deconvolution problem. This is removed by band pass-filtering. Figure 2.3 shows the deconvolution results using filter length 150 ms and gap length 8 ms on the marine shot gather.

2.1.4 Radon Demultiple

Multiple attenuation is one of the major challenge in Marine Seismic Processing. At any given time, multiples tend to have more moveout than primaries. Based on this fact, NMO correction and stack based on primary velocities should eliminate multiples. However, many multiples in marine data are too strong and sometimes the moveout differences are not large enough such as that simple stacking does not properly attenuate them.

Radon demultiple operates on this moveout differences and transforms the NMO corrected CDP gather from time domain to the parabolic radon domain. In this domain, we can model the signal and multiple noise based on the user defined primary and multiple moveout ranges. Figure 2.4 shows the demultiple result on cdp gather.

2.1.5 Kirchoff Time Migration

Migration is a process used to move dipping reflectors to their correct subsurface positions (Yilmaz 2001). It also collapses diffractions and increases spatial resolution of seismic data. The result of migration can be seen as a true approximation of the earth subsurface image, which makes it one of the most important process in seismic processing. The migration method used in this work is Kirchoff Time Migration, which is based on diffraction summation or summation of amplitudes along hyperbolic paths and incorporates wavelet shaping factors, spherical spreading, and obliquity (Yilmaz 2001). The range of amplitude summation in the Kirchoff Time Migration is called the migration aperture, whose value increases with depth. In theory, the larger aperture of migration, the better results it gives, although with limited acquisition offset, large aperture value can induce dipping artifacts especially at deep section. Pre-stack Kirchoff Time Migration has the advantage that it can handle conflicting dips with different stacking velocities better than post-stack migration (Yilmaz 2001). It also gives better velocity estimation from the migrated gathers. Such advantages makes Pre-Stack Kirchoff Time Migration widely used in the industry as it gives robust and accurate solution. Our results before and after migration shows much better imaging on small faults and structures after migration.

2.2 Non Local Means Filter

Non Local Means (NLM) filter is a next-generation signal denoising algorithm which is originally proposed for image processing (Buades, Coll, and Morel 2005) and has been used in medical imaging (Wiest-Daesslé et al. 2007) and seismic processing (Bonar and M. Sacchi 2012). The NLM filter takes the advantage of high redundancy in most natural images, which assumes for every small window in an image there are many other windows in the same image with similar structures. It takes the similarity between a neighborhood window

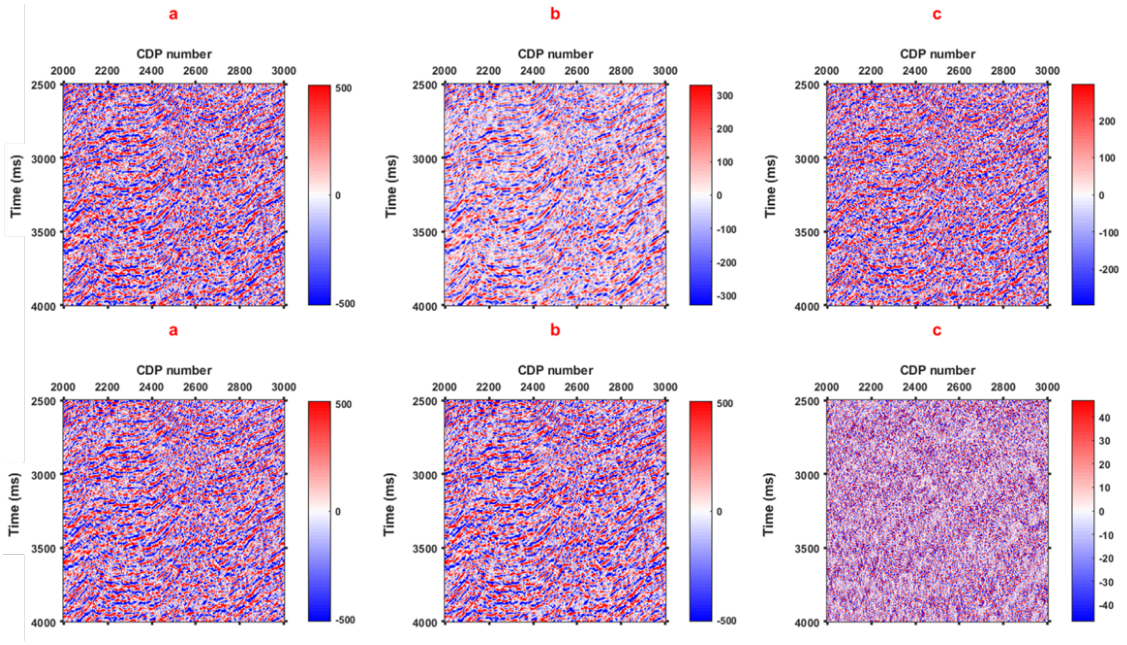

Figure 2.5: Non Local Means Filter of zoomed deep marine section using filter strength h of 0.01 (top) and 0.001 (bottom), and using a search window and neighborhood window 50 and 3 samples. (a) is input data. (b) the NLM result, and (c) the difference.

of a main pixel with other neighborhood windows within the same image to calculate the averaged value of the main pixel. It is non local because the whole image contributes to the value of the denoised pixel in consideration, not just the neighborhood of the pixel. In practice, using the entire image for search window can became very computationally demanding and thus the process is restricted within a determined search window.

A Seismic reflection image is the prime example of natural image with high redundancy, as there are lots of periodic structures and reflection packages within a seismic image. NLM filter demonstrates the ability to strongly enhance signal-to-noise ratio with high edge preservation ability (Buades, Coll, and Morel 2005) , which is suitable for denoising a seismic image. The common methods for post-stack seismic random noise attenuation such as f-x deconvolution (Canales et al. 1984), Cadzow filter (Trickett et al. 2008), and other coherency based filtering use a linearity assumption of seismic events and usually results in smearing of edges and small features, and sometimes do not handle steep reflections very well. Therefore, NLM filter is a suitable alternative for seismic denoising method, especially for imaging geothermal reservoir where faults and fractures are important features.

The implementation of NLM algorithm in this research is based on the original concept by Buades (Buades, Coll, and Morel 2005), it implementation on seismic image (Bonar and M. Sacchi 2012), and program developed in TNO (Carpentier and Steeghs 2016).

Let the discrete imaged be defined as u(i,j), the main pixel in which we are trying to find its new denoised value have coordinate (i,j) and the comparative pixels in the search window have coordinate (k,l). If we take a radius L of the search window, the NLM output or the new value of the main pixel is the weighted average sum of all pixels within the search window which is given by the equation 2.1

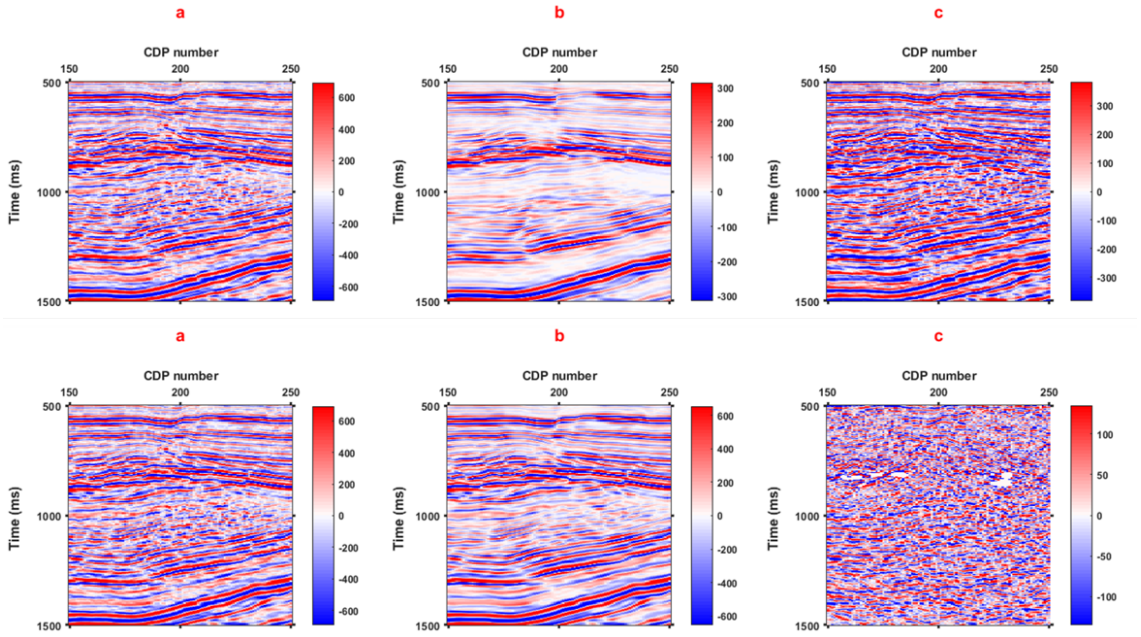

Figure 2.6: Non Local Means Filter of zoomed land section using filter strength h of 0.001 (top) and 0.00003 (bottom), and using search window and neighborhood window 50 and 3 samples. (a) is input data. (b) the NLM result, and (c) the difference. Note that it has worse performance using a similar window of 0.001 compared to the marine data. A Filter strength of 0.00003 is found to be the optimum parameter for good filtering performance without destroying much signals.

$$NLu(i,j) = \sum_{k=1-L,i=j-L}^{i+L,j+L} w(k,l)u(k,l) \tag{2.1}$$

Where the weight $0 <= w(k,l) <= 1$ of the comparative pixel in the search window is calculated based on the similarity measurement between the neighborhood of main pixel (i,j) and comparative pixel (k,l), in which the similarity is computed by its Gaussian Euclidian distance ($\|v(Ni) - v(Nj)\|_2^2$). It gives the sample closer to the main pixel inside the neighborhood window to have more significance in the similarity measurement. $Z(i)$ is normalization factor to make sure the value of $\Sigma w(k,l) = 1$ The weight calculation is given in the equation 2.2.

$$w(i,j) = \frac{1}{Z(i)} e^{-(\|v(Ni)-v(Nj)\|_2^2)/(h^2)} \tag{2.2}$$

The decay of the exponential function as a function of the Euclidean distance is controlled by the parameter h or the user defined filter strength (equation 2.2). Large value of h will assign similar weights to all j pixels in the image and small value will assigned larger weights to only a select few of j pixels in the image. If all j pixels have similar weights, the NLM algorithm become less selective which results in strong but worse performing filter. Compared to search window and neighborhood window, h is the most data dependent parameter as it performance depends on the noise level and the amplitude variance of the data. The basic rule regarding h parameter (Bonar and M. Sacchi 2012) is that the value has to be at least 0.1 times the

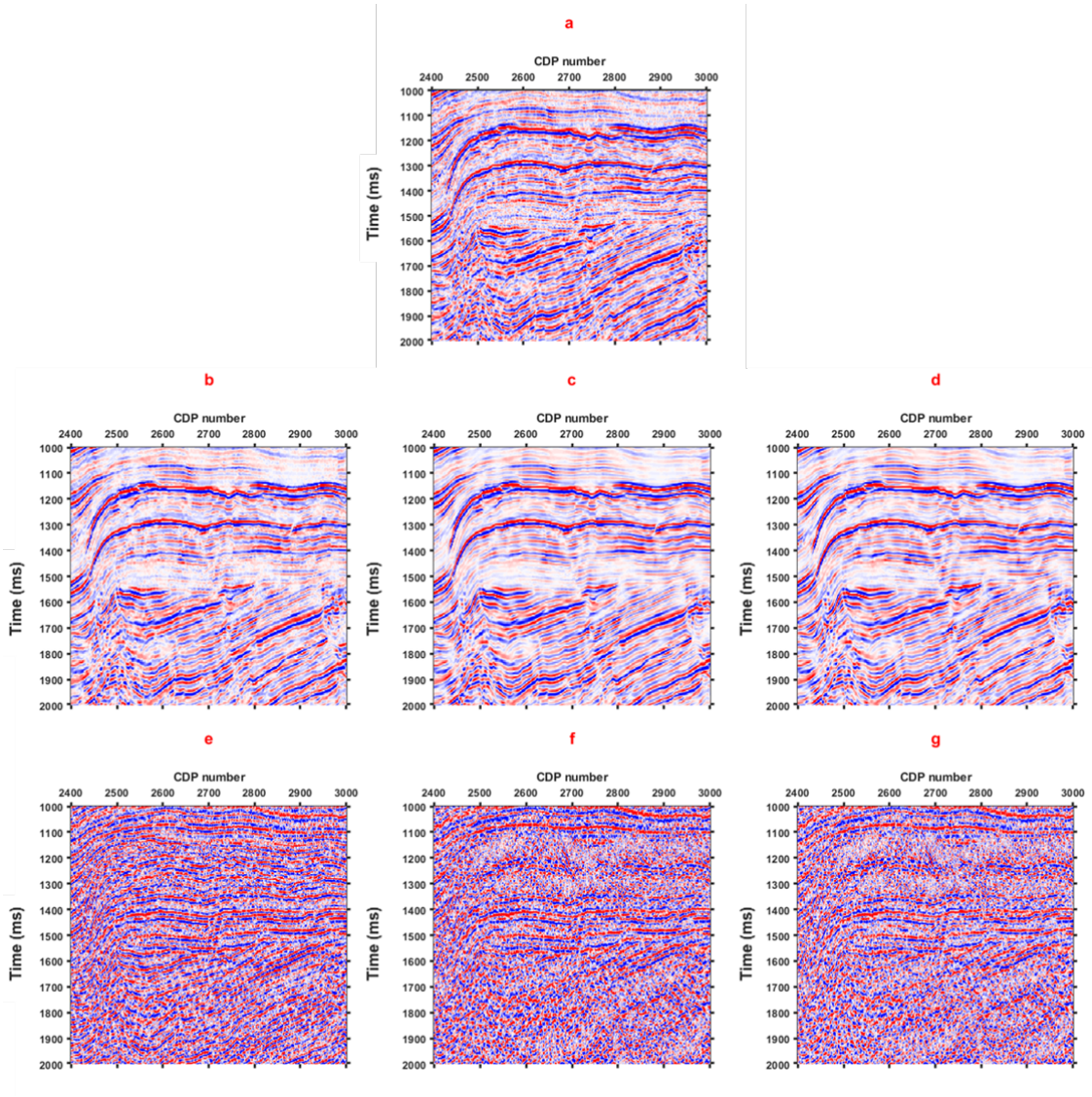

Figure 2.7: Results comparison using NLM of a) input marine data and results with 3 different neighborhood window size b) 1, c) 9, d) 19 and the difference between input data and results using results different neighborhood window size e) 1, f) 9, g) 19. The difference comparison shows using small window size of 1 filtered lots of reflective signal. Using larger than 9 shows no significant improvement

maximum amplitude in the data. Careful choice regarding the h parameter needs to be taken, especially in land data with lower signal to noise ratio as a large h value can introduce artifacts. We found that in general we need different h values between marine and land seismic data.

Figure 2.5 shows that using a larger h value of 0.01 on the GNL19-112 marine data results in stronger and less selective filtering compares to h value of 0.001. For MZ81-15 land data (Figure 2.6) we chose h parameter smaller than on the marine data in the order up to $10^{-}2$ to prevent over smoothing and artifacts.

In this research, the search window size for NLM application on both lines are chosen to be rectangular 50 x 50 samples. A larger search window will provide better results due to more information to acquire from

an image in the expense of increase in computational time. For 2D dataset, choosing a larger window than 50 x 50 is computationally expensive and does not provide significant result improvements.

Neighborhood or similarity window size needs to be chosen such it large enough to recognize structures which we want to be preserved. In seismic data, this means we have to use neighborhood window larger than the largest wavelength length in time domain (Bonar and M. Sacchi 2012). We found the optimum parameter for neighborhood window 3 to 9 for both land and marine data, and results comparison between the two n window is shown in Figure 2.7. Our testing found that after certain length, an increase in search window does not improved filtering performance, and then at certain length it starts to decrease the performance and became less selective. 2.7. shows the results comparison using different neighborhood window of 1,9, and 19

2.3 Sparse Spike Deconvolution

In mathematics, deconvolution is a process used to reverse the effects of convolution and widely used in signal and image processing. In signal processing, deconvolution refers to the problem of estimating the unknown input to an LTI (Linear Time Invariant) system when the output signal and system response are known. In theory, deconvolution is a straightforward process which involves designing inverse filter and gives exact answers. In practice, many systems such as seismic reflection are non-invertible or nearly non-invertible (ill-posed). The use of simple and straight exact inverse filters in the ill-posed inverse problem is very unstable and will greatly amplify the noise.

In reflection seismology, deconvolution is one of the important steps in digital seismic processing. Besides compressing the basic wavelet in seismogram, deconvolution is also used to eliminate reverberations and short period multiples (Yilmaz 2001). Based on the convolution model of reflection seismology, a seismogram is the sum of the convolution of source wavelet with the reflectivity coefficients and additional noise. Mathematically, it is given by:

$$y(t) = w(t) * r(t) + n(t) \tag{2.3}$$

where $y(t)$ is the recorded seismogram, $w(t)$ is the source wavelet, $r(t)$ is the earths subsurface reflectivity coefficients, $n(t)$ is noise, and $*$ denotes a convolution process. The convolution model assumes that the earth subsurface can be represented by a set of planar layers with constant acoustic impedance. In this research, the wavelet is assumed to be known, which will be acquired by estimation from seismogram.

The main purpose of deconvolution in seismic data processing is to acquire the accurate representation earths reflectivity coefficient (r(t)) to get a realistic and accurate image of the earths subsurface. From the equation 2.3 we can see that the presence of noise make the deconvolution of seismic data non-unique. Also due the fact that a seismic source wavelet and the data are always band limited, seismic deconvolution is an ill-posed inversed problem which produces limited band-width results.

To solve the non-uniqueness problem of seismic deconvolution, the approach is to pick a solution that (1) fits the data and (2) satisfies a given set of constraints (Velis 2007). The approach for (1) is to minimize the data error and (2) to add prior information about the data to discard implausible models by a method called regularization (Tarantola 2005). The conventional method of predictive Wiener deconvolution in seismic

data processing uses ℓ_2 norm regularization (Tikhonov 1963) in the inversion to suppress noise disturbance, which results in frequency band-limited reflectivity coefficient approximation.

In sparse spike deconvolution, the prior information is the assumption of earth reflectivity as a sparse sequence of spikes. This assumption is due to the fact that the bigger reflectivity coefficients are the main contributors of acoustic impedance, which can be seen as spatially spaced geological boundaries. By adding a sparsity constraint as prior information about reflectivity in the inversion, an approximation of the correct amplitude and location of the sparse reflectivity series can be obtained, and significant increase in bandwidth content can be achieved from band-limited seismic observations.

There are several methods for adding sparse constraint in inversions, the common method use is the optimization of a norm that forces sparse solution (Chapman and Barrodale 1983; Debeye and Van Riel 1990; M. D. Sacchi, Velis, and Cominguez 1994). In this research, this is done by non quadratic optimization of ℓ_1 norm regularized inversion (Taylor, Banks, and McCoy 1979) of seismic data and estimated source wavelet (Chapman and Barrodale 1983), with the half quadratic approach to solve the minimization problem of ℓ_1 norm, based on method done on SAR imaging (Mujdat Cetin, Karl, and Castanón 2003) and image processing (He et al. 2014). To preserve reflection amplitudes and impose lateral continuity of seismic data, we added ℓ_2 norm smoothness derivative constraints in the cost function. At last, to fix the common problem of high frequency noises of ℓ_1 norm regularized deconvolution, we applied the Non Local Means Algorithm(Buades, Coll, and Morel 2005) before deconvolution to increase the signal to noise ratio while preserving fault edges.

2.3.1 Theory

To illustrate how we approach this problem, lets take a look at a discretized or matrix version of the seismic convolution model in the equation 2.3 as

$$y = Wr + n \tag{2.4}$$

where y is a sampled seismic data, r is the earth reflectivity coefficient, W is the estimated source wavelet matrix, and n is noise. A solution to the problem of estimating the earth true reflectivity coefficient can be obtained through a generalized least squares solution:

$$r_{LS} = argmin\|y - Wr\|_2^2 \tag{2.5}$$

and cost function or data error function is given by

$$J(r) = \|y - Wr\|_2^2 \tag{2.6}$$

where $\|.\|_2^2$ denotes the ℓ_2 norm. The generalized least square solution aims to find the r value (r_{LS}) which will minimize the squared error or ℓ_2 norm error of the actual observations (y - Wr). As we discussed before about the ill-posed inverse problem, the generalized least squares solution is unstable due to noise perturbation. To overcome this problem, a regularization can be done by allowing the inclusion of prior information to get a stable solution in the presence of noise in the data.

A commonly used regularization is Tikhonov regularization (Tikhonov 1963), in which the inclusion of prior information is done by adding the additional regularization term in the cost function as follows:

$$J(tik) = \|y - Wr\|_2^2 + \lambda^2 \|Pr\|_2^2 \tag{2.7}$$

where λ is regularization parameter and its value controls the trade off between the first and second term of the equation. The first term is the data fidelity term and the second term is the regularization term which includes the prior information. The common choice to use for P is an identity matrix, which then acts to penalize large values of the solution and reduce noise amplification or Derivative matrix which impose smoothness to the solution (Mujdat Cetin, Karl, and Castanón 2003). The linear equation for the Tikhonov analytical solution can be written as:

$$(W^T W + \lambda^2 P^T P)\, r_{TIK} = W^T y \tag{2.8}$$

Which gives a quadratic solution of r (r_{TIK}). The advantage of quadratic regularization or ℓ_2 norm regularization is that it results in linear solutions which are computationally easy to solve. The disadvantage is that it results in a smoothed image and blurred sharp boundaries. To impose a sparsity constraint or sparse prior information in the inversion, we use an ℓ_1 norm regularization instead of ℓ_2 regularization, which sometimes is called Total Variation Regularization (Rudin, Osher, and Fatemi 1992). The usage of ℓ_1 norm regularization to obtain a sparse solution and edge preserved images has been demonstrated in many applications such as astronomy (Geman and Yang 1995), medical imaging (Y. Wang and Zhou 2006), SAR imaging (M Cetin n.d.) and seismic deconvolution (Chapman and Barrodale 1983). The ℓ_1 norm regularization cost function is given by equation 2.9

$$J(TV) = \|y - Wr\|_2^2 + \lambda^2 \|Pr\|_1 \tag{2.9}$$

The cost function of ℓ_1 norm in the equation 2.9 is non-differentiable which leads to challenging nonlinear optimization problem (Bovik 2010). To solve the non-differentiable property of ℓ_k norm when $k \leq 1$, one of the approaches is to use a smooth approximation of the solution (Acar and Vogel 1994) given by:

$$\|r\|_k^k = \sum_{i=1}^{N} ((r_i)^2 + e)^{\frac{k}{2}} \quad \text{or when } k = 1\,, \quad \|r\|_1 = \sum_{i=1}^{N} \sqrt{(r_i)^2 + \epsilon} \tag{2.10}$$

where $\epsilon > 0$ is a small constant, N = length of vector, and i denote r at its i th element. If we take a diagonal matrix $\Lambda(r)$ which depends on r and ϵ as given by:

$$\Lambda(r) = \frac{1}{2}\, diag \frac{1}{\sqrt{(r_i)^2 + \epsilon}} \tag{2.11}$$

The solution of the equation 2.9 (Bovik 2010) becomes:

$$(W^T W \,+\, \lambda^2\, P^T\, \Lambda(r)\, P)\, r_{TV} = \, W^T y \tag{2.12}$$

Which gives the analytical solution of r (r_{TV}). Note the equation 2.12 is equal to equation 2.8 when $\Lambda(r) = 1$. Although the equation 2.12 is still nonlinear due to diagonal matrix dependency on r, it is found it can be solved by simple fixed point iteration (Bovik 2010) of a linear equation for r given by the equation:

$$(W^T W + \lambda^2 P^T \Lambda(r^{(n)} P)\, {r_{TV}}^{(n+1)} = W^T y \quad n = 0, 1, ... \tag{2.13}$$

Which can be solved by quasi-Newton method:

$${r_{TV}}^{(n+1)} = {r_{TV}}^{(n)} - [H(r^n)]^{-1} \bigtriangledown (r^n) \tag{2.14}$$

where $H(r^n)$ is the Hessian or second derivative matrix of r and $\bigtriangledown(r^n)$ is the first derivative matrix of r. The problem with this approach as stated by Vogel et al (Vogel and Oman 1998) for ℓ_1 norm minimization is that standard non linear method such as Newton's method or quasi-Newton's tend to perform poorly for ℓ_1 norm regularization. One of the approach to solve this is by half-quadratic regularization (Geman and Yang 1995; Vogel and Oman 1998). In this research, we will use half-quadratic regularization method developed by M Cetin et al (M Cetin n.d.) which proven to give more efficient and robust solution of ℓ_1 norm minimization.

2.3.2 Smoothness constraints and Half Quadratic Optimization

We use Half-quadratic regularization (M Cetin n.d.) and impose smoothness constraint in the cost function of equation 2.16 in the form of discrete derivative operator matrix D, which is given by:

$$D = \begin{bmatrix} -1 & 1 & & & \\ & \ddots & \ddots & & \\ & & \ddots & \ddots & \\ & & & -1 & 1 \end{bmatrix} \tag{2.15}$$

The additional regularization term aims to preserve reflection structures and amplitude, which is important for seismic interpretation. The resulting cost function with added smoothing constraint is given by:

$$J(r) = \|y - Wr\|_2^2 + \lambda 1^2 \|r\|_{k1}^{k1} + \lambda 2^2 \|Dr\|_{k2}^{k2} \tag{2.16}$$

One of the approach is to use the same value of k for both terms with $k1 = k2 = 1$ (M Cetin n.d.). We found that using $k1 = 1$ and $k2 = 2$ gives best results for maximum resolution and smoothness of seismic data. The parameters $\lambda 1$ and $\lambda 2$ control the trade-off between data error minimization, sparsity constraints, and smoothness constraints. By using the same smoothness approximation of the solution as in the equation 2.10, the equation 2.16 can be written as:

$$J(r) = \|y - Wr\|_2^2 + \lambda 1^2 \sum_{i=1}^{N} ((r_i)^2 + e)^{\frac{k1}{2}} + \sum_{i=1}^{N} ((Dr_i)^2 + e)^{\frac{k2}{2}} \tag{2.17}$$

The first derivative or gradient of the equation 2.17 is given by:

$$\bigtriangledown J(r) = 2W^T Wr \; + \; k1\lambda_1^2 Q1\, r\Lambda_1(r) \; + \; k2\lambda_2^2 D^T \Lambda_2(r) D \tag{2.18}$$

The compact gradient form of equation 2.17 can be written as:

$$\bigtriangledown J(r) = H(r) - 2W^H y \tag{2.19}$$

where the Hessian matrix approximation is given by:

$$H(r) \triangleq 2W^T W \; + \; k1\lambda_1^2 \Lambda_1(r) \; + \; k2\lambda_2^2 D^T \Lambda_2(r) D \tag{2.20}$$

and we take the same diagonal matrix as in equation 2.11 times two for both regularization terms:

$$\Lambda_1(r) \triangleq \; diag\left[\frac{1}{((r_i)^2 + \epsilon)^{1-\frac{k1}{2}}}\right] \tag{2.21}$$

$$\Lambda_2(r) \triangleq \; diag\left[\frac{1}{((D\, r_i)^2 + \epsilon)^{1-\frac{k2}{2}}}\right] \tag{2.22}$$

Because we will use $k2 = 2$ for smoothing constraint, the diagonal matrix $\Lambda_2(r)$ will be equal to 1.

We use quasi-Newton iteration to solve r from the Hessian $H(r)$ approximation based on the method by M Cetin et al (M Cetin n.d.) given by:

$$r^{n+1} = r^n \; - \; \gamma\big[H(r^n]^{-1} \; \bigtriangledown \, J(r^n) \tag{2.23}$$

where γ is step size. Substituting the equation 2.19 to equation 2.23 gives the iterative algorithm:

$$H\big(r^n\big)r^{n+1} = (1-\gamma)H\big(r^n\big)r^n \; + \; \gamma 2W^H y \tag{2.24}$$

This equation results in the coefficient matrix of $H(r^{(n)})$ which is sparse, Hermitian, and positive semi definite (M Cetin n.d.), which can be solved iteratively by Conjugate Gradient method to find the find $(r^{(n+1)}$. If we take:

$$v = (1-\gamma)H\big(r^n\big)r^n \; + \; \gamma 2W^H y \tag{2.25}$$

The conjugate gradient scheme can be written as:

$$H\big(r^n\big)r^{n+1} = v \tag{2.26}$$

And the iteration is run until $\|r^{(n+1)} \; - \; r^{(n)}\|_2^2 \,/\, \|r^{(n)}\|_2^2 \; < \; \delta$ where $\delta > 0$ is a small constant, which in this research the chosen value of δ is $1 * 10^{-7}$. The iterative algorithm scheme (Mujdat Cetin, Karl, and Castanón 2003) is shown in figure 2.8.

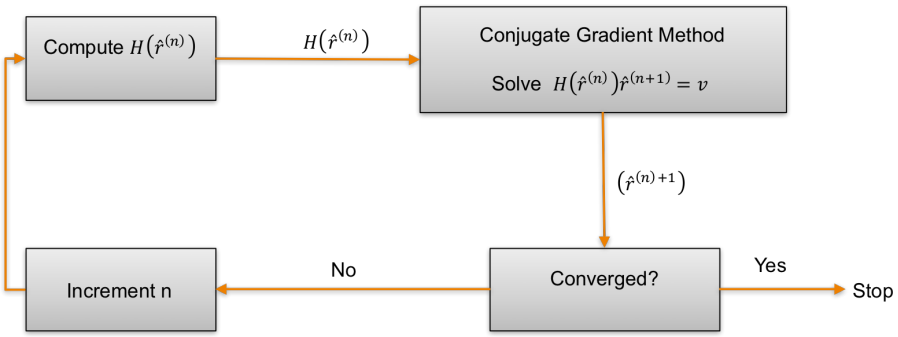

Figure 2.8: Quasi Newton based iterative algorithm scheme (Mujdat Cetin, Karl, and Castanón 2003)

2.3.3 Wavelet Estimation

To solve the inverse problem of seismic deconvolution in the equation 3, seismogram r and source wavelet W are needed. The source wavelet of seismic reflection is mostly not known, but it can be estimated from seismic data. The main idea behind seismic wavelet estimation is based on the fact that the smoothed amplitude spectra of source wavelet has similar shape, in fact is almost indistinguishable from the source wavelet amplitude spectra (Yilmaz 2001).

In this research, a multi traced windowed approached is done to estimate the source wavelet. Using the selected time window, for every trace the amplitude spectra of traces around the main trace are smoothed and averaged. The sum of those smoothed spectra are inverted back to time using inverse Fourier transform to get the estimated source wavelet. Using this method, we obtained a smoothed spatially varying and depth targeted source wavelet to prevent noise amplification which results from non smooth wavelet.

Due to the fact that most of seismic data frequency bandwidth are depth dependent, selecting different time window means different source wavelet which will give different inversion results in terms of noise level. We found that using $\ell_2(r)$ norm smoothing constraint and/or Non Local Means Algorithm before deconvolution helps reduce such effect.

2.3.4 Sparsity and Smoothness Regularization Parameters

Figure 2.9 shows the result of a single trace sparse spike deconvolution with $\lambda_2(r) = 0$ or without any smoothing constraints to test the effect of different $\lambda_1(r)$ parameter. We found that using small value of $\lambda_1(r) = 0.5$ already produces a sparse solution. We found that using higher value of $\lambda_1(r) = 0.9$ and $\lambda_1(r) = 5$ does not effect the amplitude and position of the sparse solution significantly.

Figure 2.10 shows the result of sparse spike deconvolution with added smoothness derivative constraint. Our test shows that using k=2 for derivative smoothness constraint or $\ell_2(r)$ norm produces better results in terms of sparsity and smoothness compared to $\ell_1(r)$ norm derivative constraint. It still shows multiple reflection packages emerges while the added smoothness constraints preserves reflection packages amplitudes and structures. The results on multiple traces real data will be shown in the next chapter.

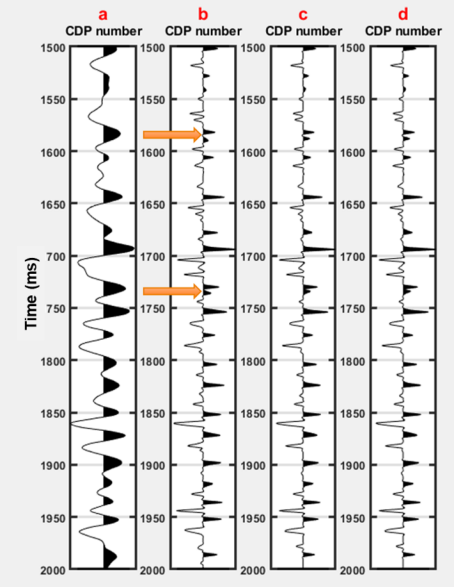

Figure 2.9: Comparison of using different λ_1 value for sparsity constraints of a) input data and b) $\lambda_1 = 0.5$ c) $\lambda_1 = 0.9$, and d) $\lambda_1 = 5$. The orange arrow shows two reflection packages emerge from single reflection package after sparse deconvolution

2.3.5 Non Local Means Algorithm to prevent noise artifacts in deconvolution

If the sparse spike deconvolution is exactly regularized and weighted, the artifacts effect caused by random noise is diminished (Velis 2007). Moreover, artifacts due to instability due to noise disturbance remains a challenge in sparse inversion. Some solutions of this problem include a spatial smoothness constraint in the inversion (J. Wang, X. Wang, Perz, et al. 2006), frequency-space (FX) weighted -filtering applied to the inverse matrix in multi-channel sparse deconvolution (J. Wang and M. Sacchi 2008), random noise filtering (FX) applied before deconvolution (Karslı, Güney, and Senkaya 2017). In this research, an approach similar to the third approach is used; more precisely by applying Non Local Means (NLM) filter before sparse spike deconvolution.

The usage of adaptive Non Local Means filtering for random noise attenuation with strong edge preservation properties are expected to bring improvement over the commonly used random noise filtering method like FX filtering, and thus reduce the artifacts caused by noise disturbance but maintaining edge preservation for further fault and fracture interpretation. The results of sparse deconvolution after NLM will be shown in the next chapter.

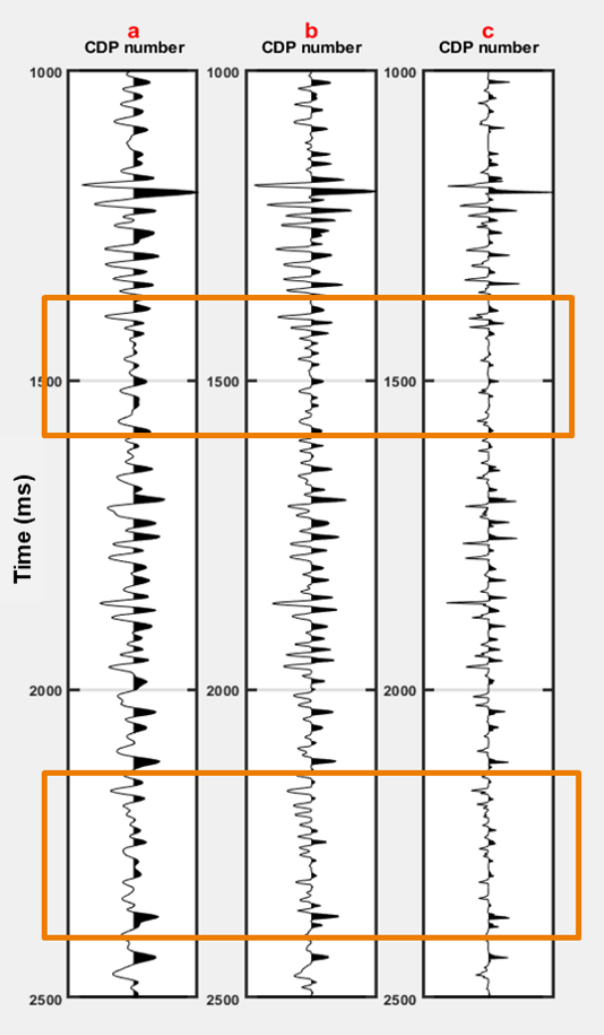

Figure 2.10: Comparison of using different k vale for smoothness contsraints of a) input data = b) $k = 2$, c) $k = 1$. Orange boxes shows particular area where we can see better results on $k = 2$ smoothing constraint compared to the $k = 2$ results

3 Results

To illustrate the conventional seismic processing, Non Local Means Algorithm and Sparse Spike deconvolution performance on a real data set, the results are shown in this chapter. The real data set used are marine line GNL91-112 and land line MZ85-15, with the position shown in Figure 2.1. In the end, the results and especially the sparse spike deconvolution performance are evaluated using well seismic tie from surrounding wells.

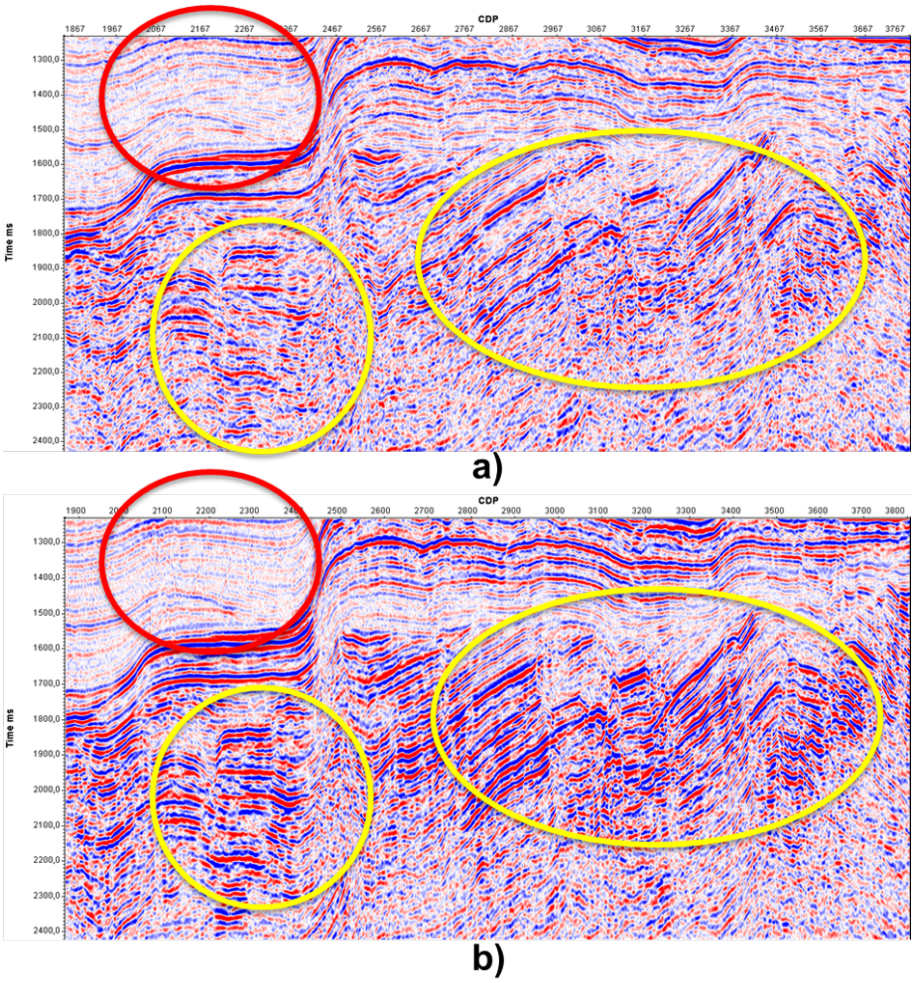

Figure 3.1: The comparison between zoomed section of offshore dataset GNL19-112 old section (top) and after reprocessed (bottom). The old section is post-stack time migrated and the reprocessed section is pre-stack time migrated. Note the improvement on the reflectors continuity and fault delineation on the yellow circle. The red circle shows the superior demultiple results by the lack of multiple reflections on the red circle.

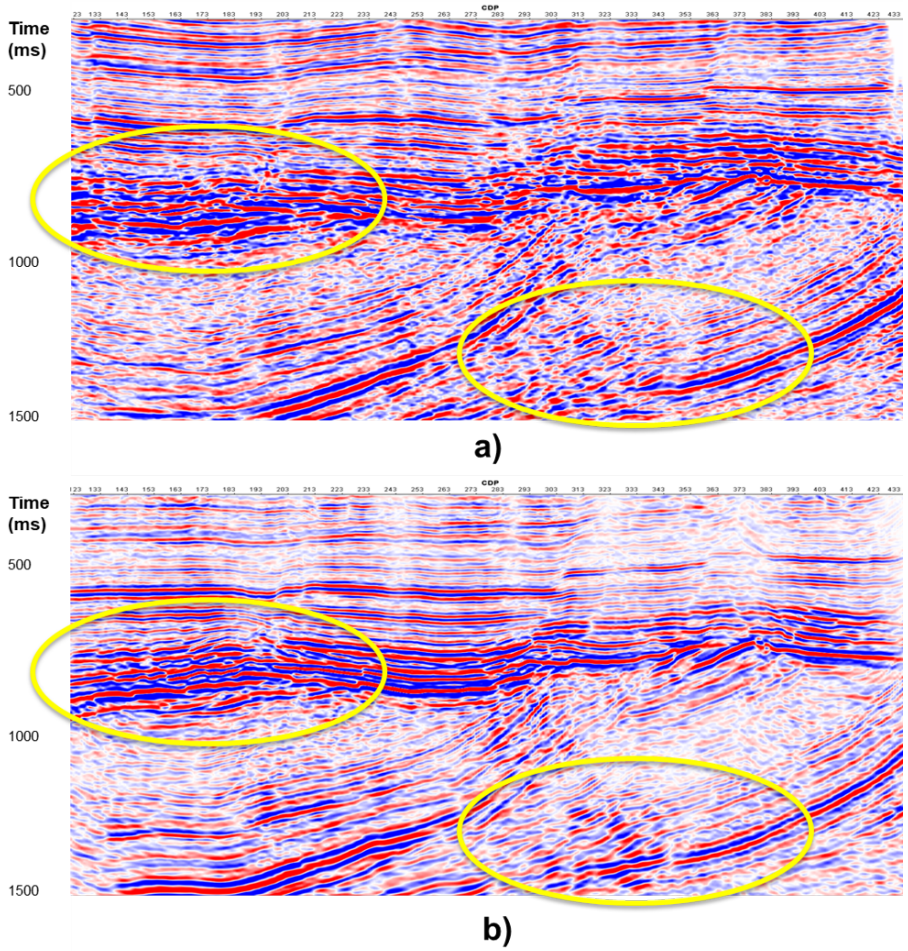

Figure 3.2: The comparison between zoomed section of onshore dataset MZ85-15 old section (top) and reprocessed (bottom). The old section is post-stack time migrated and the reprocessed section is pre-stack time migrated. Note improvements on the reflectors continuity and coherence as well as fault delineation on the yellow circle. The statics are also better shows by flatter reflectors on the shallow section.

3.1 Conventional Processing

The seismic reprocessing results using conventional workflow (Yilmaz 2001) produced improvements of the old seismic data, especially on the shallow to mid-depth reflectors, up to depth of 3000 ms as can be seen from the figure 3.1 and figure 3.3. The results are expected considering the improvement over seismic reflection processing algorithm used through the years since the processing of the old data at 1980s, especially due to the Pre-Stack Kirchoff Time Migration algorithm, demultiple on marine line and statics algorithm for the off shore line. The improvement of deep Dinantian reflectors are however, insignificant due to offset limitation caused by the acquisition offset 3500 m (Figure 3.3). With limited offset, Pre-Stack Time Migration does not have enough aperture to properly image deep reflectors. These deep reflectors improvement will be thoroughly investigated by the Non Local Means Algorithm method. These new improved reprocessed line act as a good base for testing and applying Non Local Means algorithm and Sparse Spike Deconvolution to

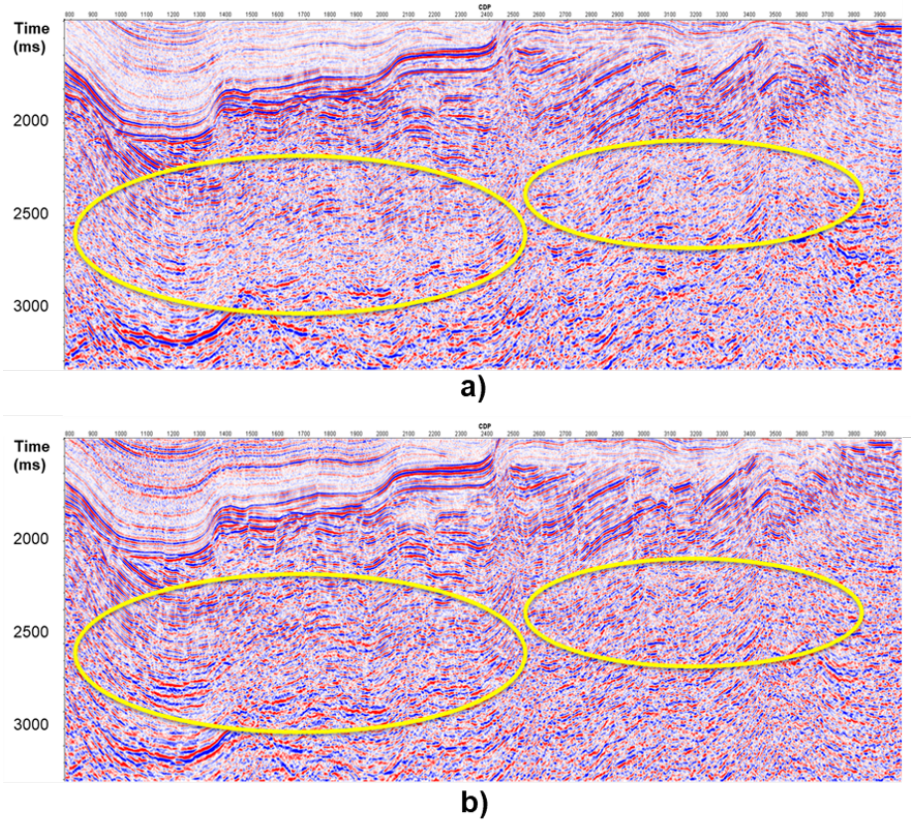

Figure 3.3: The comparison between zoomed section of offshore dataset GNL19-112 on the deep sections before reprocessed and after reprocessed. Both are time migrated sections. There are improvements on the reflectors continuity and fault delineation on the yellow circle, however its minimal.

further get better images of the geothermal reservoirs.

3.2 Non Local Means Filter

3.2.1 Off-shore Line (GNL91-112)

Figure 3.4 shows the results comparison of Non Local Means filter using different neighborhood window 3 & 9 applied on the marine line. As shown in the Methodology section in Figure 2.5, the neighborhood window size needs to be chosen larger than the seismic structures we want to be preserved (seismic wavelength length in time). As with most seismic data, the frequency of seismic data is depth dependent. We found that using a search window of 9 gives better results to resolve deep structures (figure 3.4) while for shallow structures search window of 3 is sufficient (Figure 3.5). The overall results of NLM shown highly enhanced signal to noise ratio with edges and steeply dipping reflectors preserved. However, we found that the short offset factor limiting the migration aperture still prevents us to get clear reflection of deep Dinantian formations.

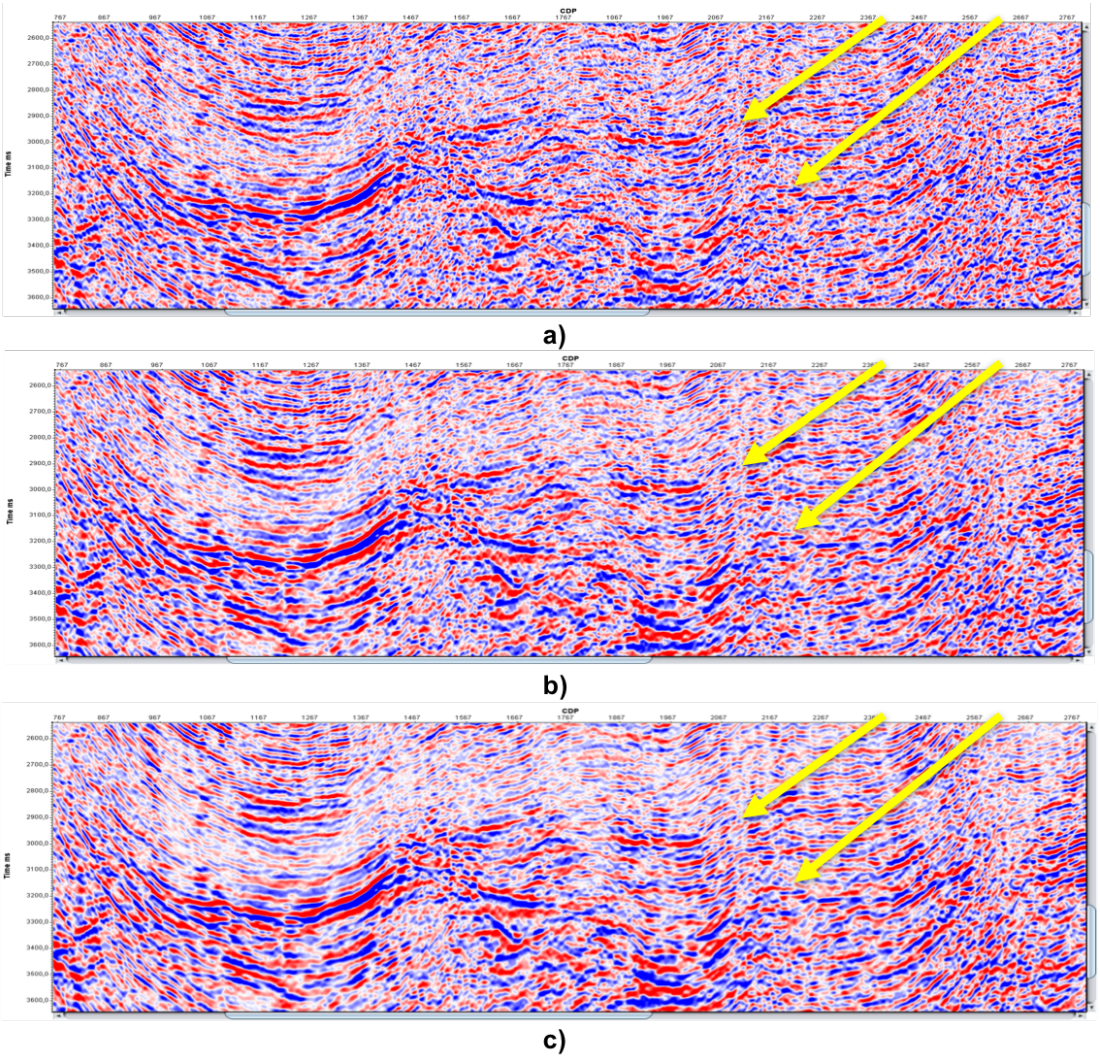

Figure 3.4: The comparison between zoomed section of offshore dataset GNL19-112 on the deep sections a) migrated section b) after NLM with $sw = 50$, $nw = 3$, $h = 0.001$ c) after NLM with $sw = 50$, $nw = 9$, $h = 0.001$. Yellow arrows point to possible Dinantian reflectors

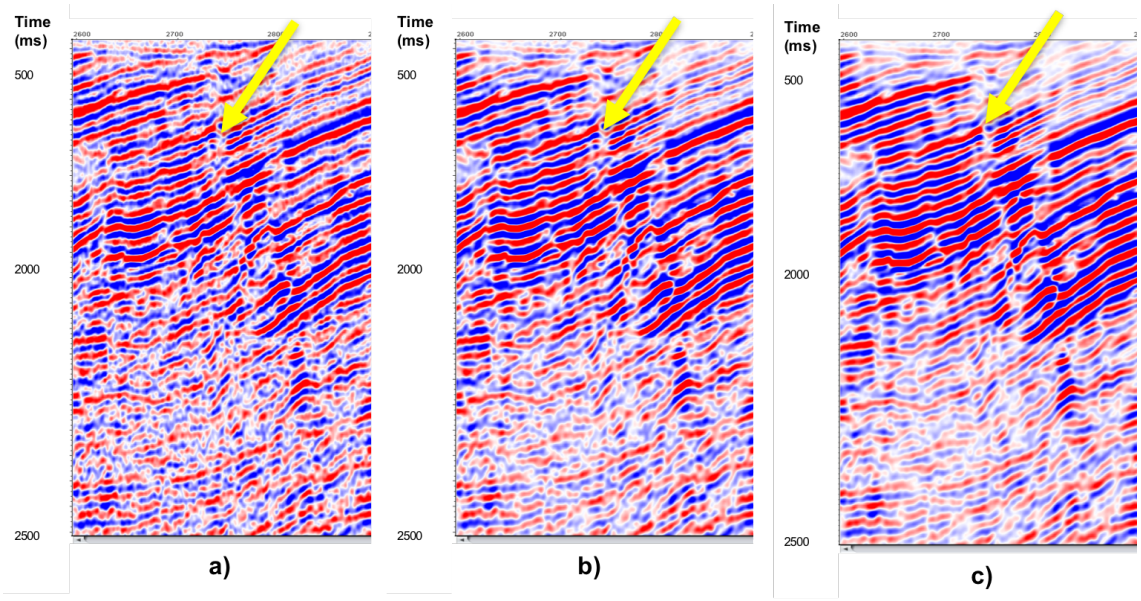

Figure 3.5: The comparison between zoomed section of offshore dataset GNL19-112 on the mid-depth sections a) migrated section b) after NLM with $sw = 50$, $nw = 3$, $h = 0.001$ c) after NLM with $sw = 50$, $nw = 9$, $h = 0.001$. Yellow arrows point preserved faults after NLM

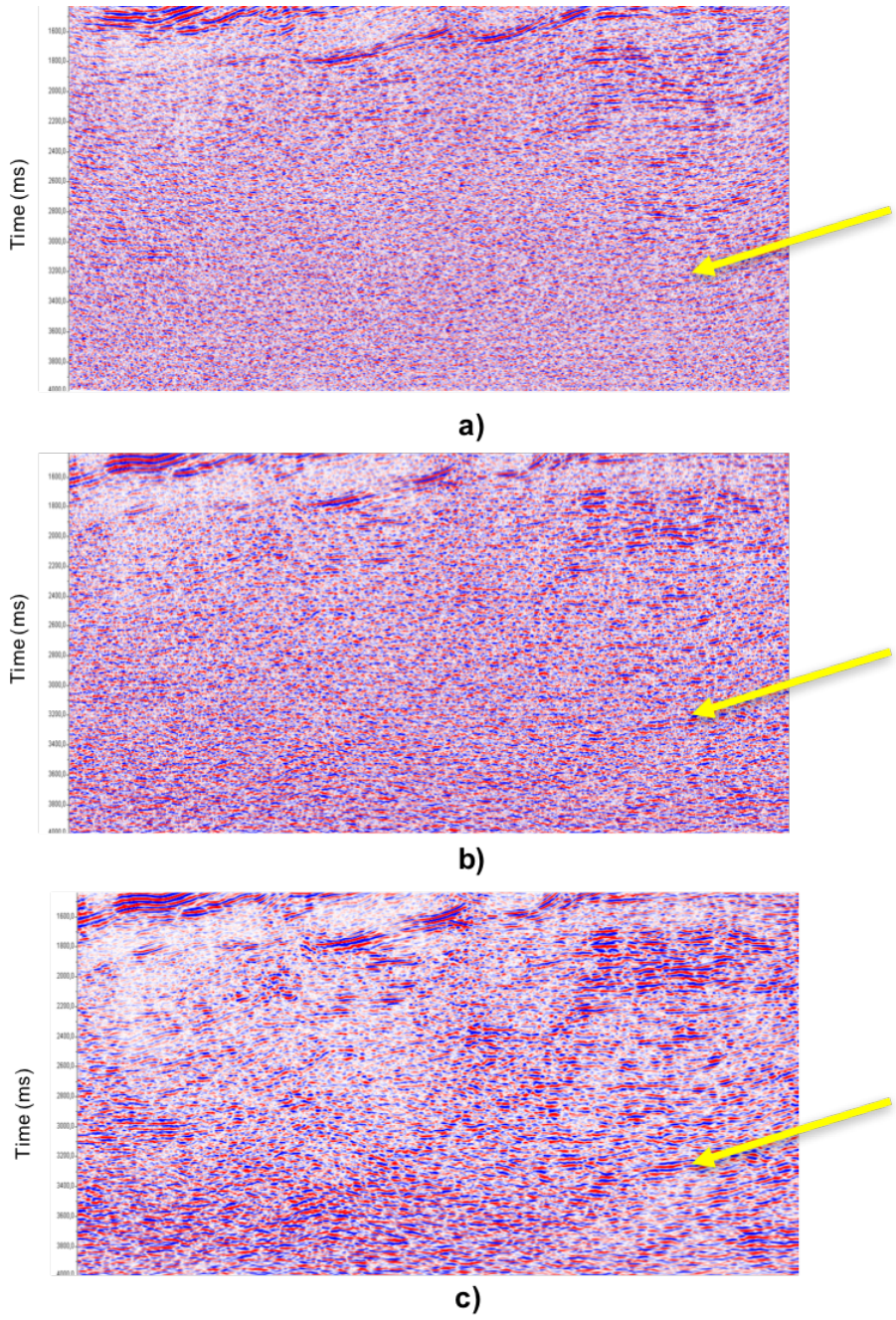

Figure 3.6: The comparison between zoomed section of onshore dataset MZ85-15 on the deep sections a) old section b) migrated section, and c) after NLM with $sw = 50$, $nw = 9$, $h = 0.0003$. Yellow arrows point to possible Dinantian reflectors

3.3 Sparse Spike Deconvolution

Sparse spike deconvolution is applied to the datasets with and without NLM filter applied to compare the effect of random noise attenuation effect on the regularized inversion. The source wavelet is estimated using a smoothed frequency spectrum of multiple traces within a chosen time window. The chosen time window is 2000 to 3500 ms to capture the source wavelet within the mid to deep reflectors. The regularization parameter λ_1 and λ_1 are tested to give optimum results. We chose $\lambda_1 = 0.9$ as it gives satisfying results in the sparse presentation of reflectivity. Figure 2.9 shown that using smaller or larger value of λ_1 does not produce a significant change in the reflection position and amplitude.

Figure 3.7 shows that the sparse spike deconvolution without smoothing constraints in the regularization produces sparse reflectivity spikes; however, such result is difficult to interpret as it is difficult to distinguish layers and structures. To preserve amplitude and structures, we impose smoothness constraint using ℓ_2 norm of derivative constraint in the regularization. For this method, we chose $\lambda_2 = 9$. The results shows the vertical resolution of the data is enhanced after sparse spike deconvolution. Moreover, with the smoothing constraint in the regularization, the structures and reflection amplitudes are preserved.

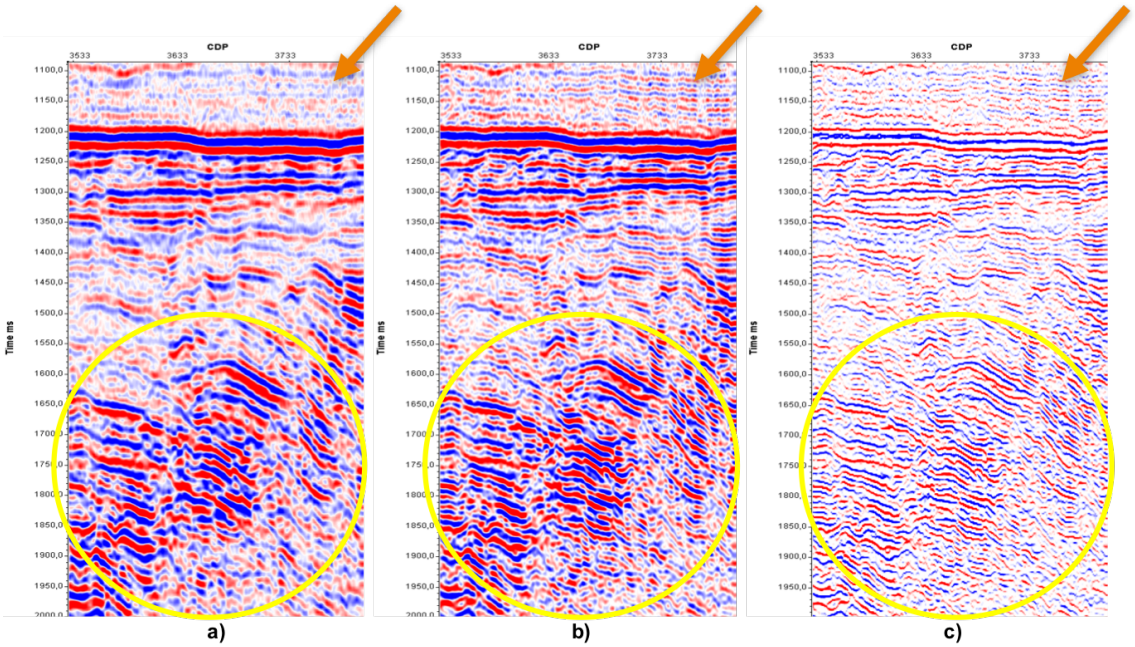

Figure 3.7: a) Zoomed migrated marine data b)after Sparse deconvolution with added ℓ_2 smoothing constraints and λ_2=9 c) after Sparse deconvolution with λ_2=0 or without any smoothing constraint.Yellow circle shows the enhanced resolution makes small structures and reflection packages emerges from the data. Orange arrow shows reflection packages emerges from noisy data

This smoothing method used is compared to the so called "post-processing" method, which can be done by either simple band-pass filter to omit high frequency spectrum or re-sampling the data from 2ms to 4ms and applying anti-aliasing filter to impose smoothness. The comparison is shown in Figure 3.8, and it shows that our method of using ℓ_2 norm derivative smoothing constraint produces results with better reflection continuity than the post-processing method. Figure 3.9 shows the result of sparse spike deconvolution after

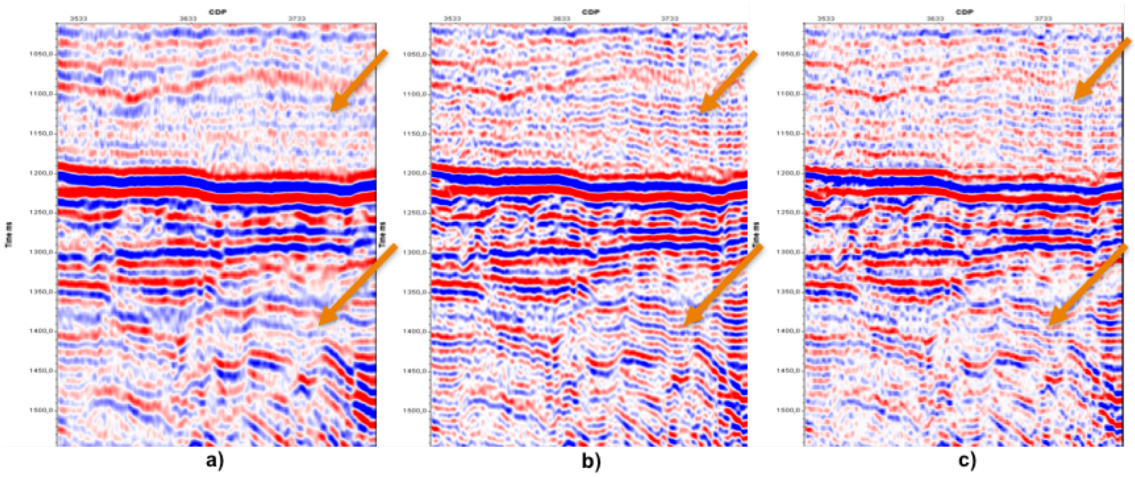

Figure 3.8: a) Zoomed migrated marine data b)after Sparse deconvolution with added ℓ_2 smoothing constraints and $\lambda_2 = 9$ c) after Sparse deconvolution with $\lambda_2 = 0$ or without any smoothing constraint and bandpass filtering applied. Orange arrows shows areas with better reflection continuity on b)

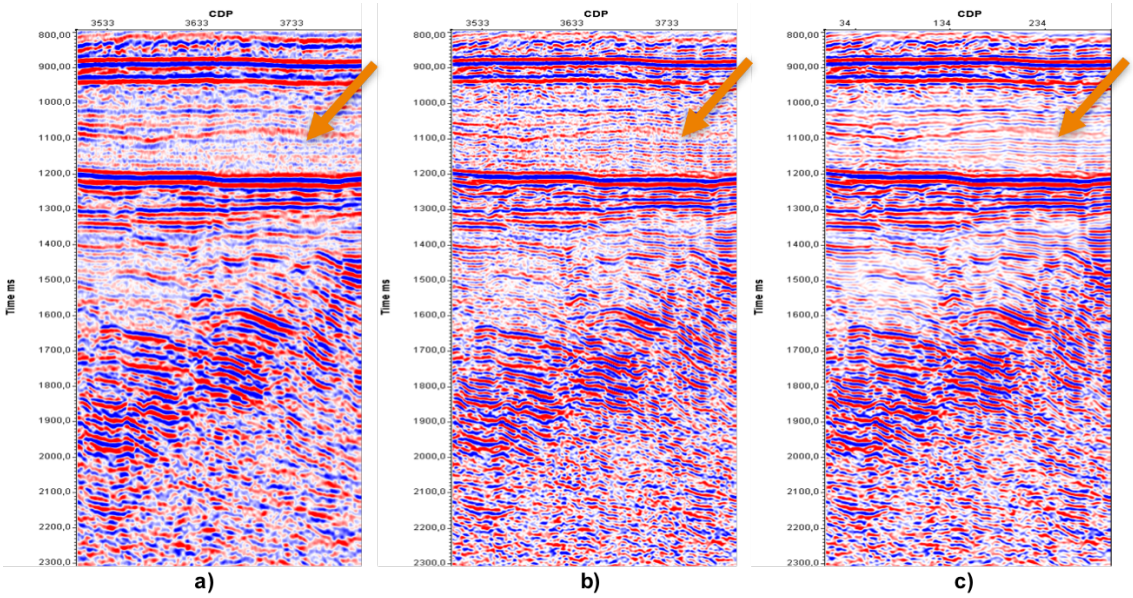

Figure 3.9: a) Zoomed migrated marine data b) after Sparse deconvolution c) after Sparse deconvolution with NLM filter applied before deconvolution. Orange arrows shows areas with better reflection continuity and signal to noise ratio on c)

NLM. It shows that sparse spike deconvolution after NLM produces results with better signal to noise ratio. The problem with high resolution deconvolution method is that it tends to give high frequency noise artifacts due to noise perturbation, and some author uses spatial smoothness in the inversion (J. Wang, X. Wang, Perz, et al. 2006) or random noise filtering (FX) applied before deconvolution (Karslı, Güney, and Senkaya 2017) to tackle the problem. Our method shows that using NLM before sparse spike deconvolution helps to reduce the noise artifacts. Due to strong edge preservation property of NLM, the fault edges are preserved.

We evaluate our results and method of the sparse spike deconvolution by doing well-seismic tie and compare the well correlation of migrated data and enhanced bandwidth data after sparse spike deconvolution. We use the closest wells of P04-01, P10-03, and P10-01 with the GNL91-112 line(Figure 3.10). The well correlation is done by synthetic seismogram generation of the sonic and density logs. Some time shifts are applied to match the reflections between seismic data and synthetic seismogram and to compensate for the offset distance of the wells to the GNL91-112 seismic line.

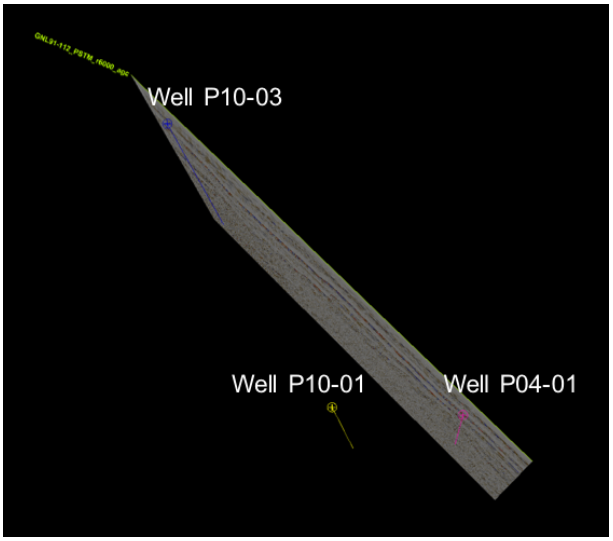

Figure 3.10: P04-01, P10-03, and P10-01 locations and GNL91-112 marine line

The well-seismic tie for the three closest wells (Figure 3.10) shows the sparse spike deconvolution stack has better well seismic-tie than the PSTM only stack (Figure 3.11,3.12,3.13). At some parts (highlighted by the yellow boxes in figures) the number of reflection packages and its position matches exactly with the synthetic seismogram.

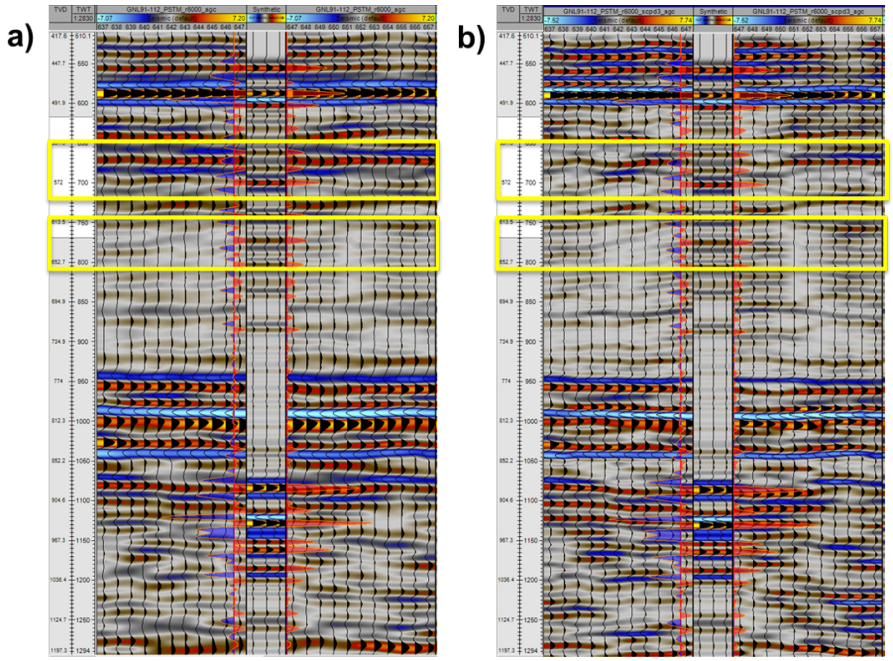

Figure 3.11: P04-01 well seismic tie with a)PSTM stack and b) sparse deconvolution stack of the GNL91-112 Marine Line.Yellow boxes shows the area of better well correlation of the sparse deconvolution stack. Time shift of well 70 ms up is applied

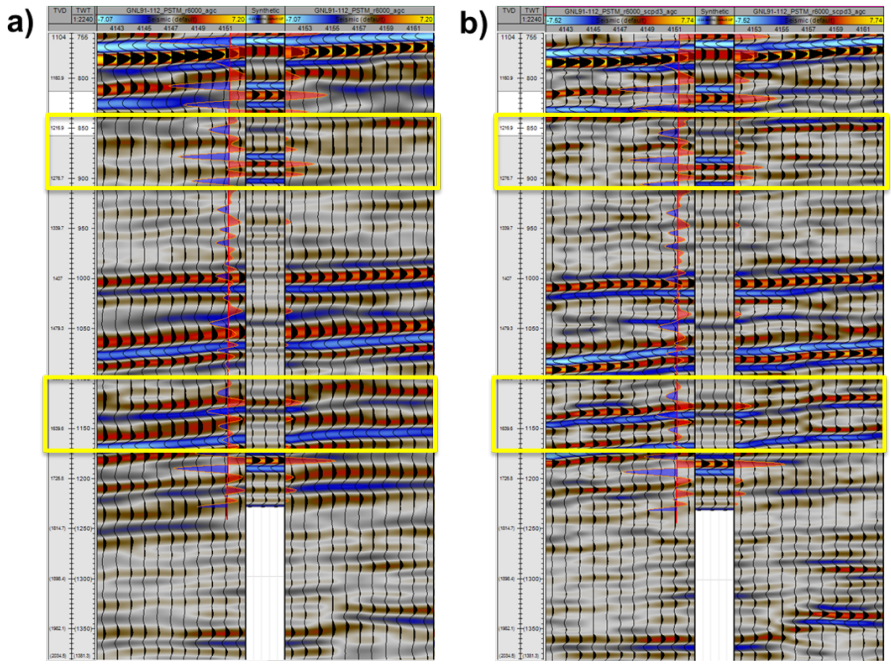

Figure 3.12: P10-03 well seismic tie with a)PSTM stack and b) sparse deconvolution stack of the GNL91-112 Marine Line.Yellow boxes shows the area of better well correlation of the sparse deconvolution stack. Time shift of well 70 ms up is applied

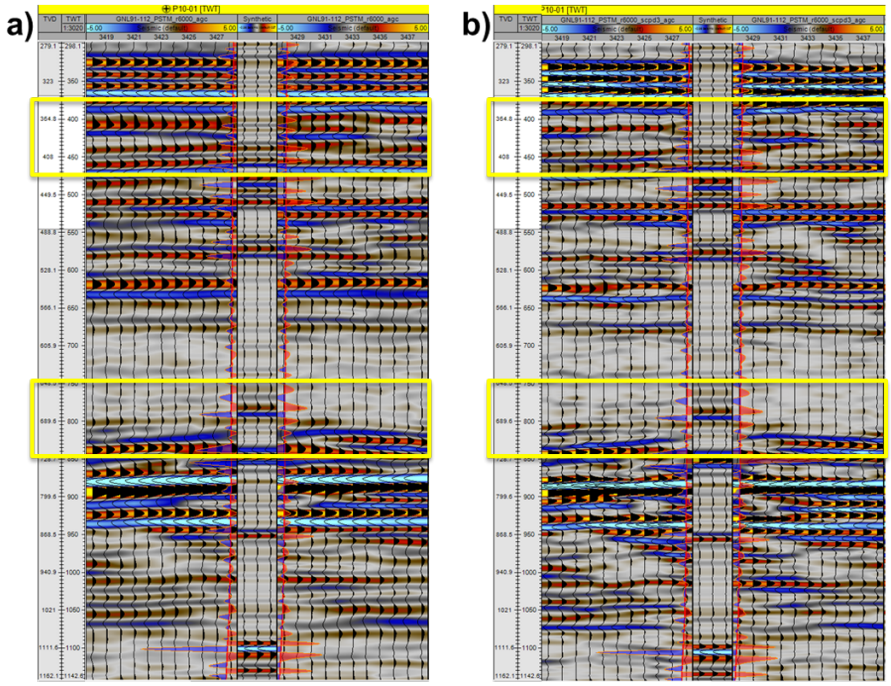

Figure 3.13: P10-01 well seismic tie with a)PSTM stack and b) sparse deconvolution stack of the GNL91-112 Marine Line.Yellow boxes shows the area of better well correlation of the sparse deconvolution stack. Time shift of well 70 ms up is applied

4 Discussion

4.1 Non Local Means and Sparse Spike Deconvolution approach for seismic processing

NLM was found to be working flawlessly in a synthetic dataset (Bonar and M. Sacchi 2012).However, the problem with real seismic data is that it has depth dependent frequency content, amplitude, and noise level. Our results with applying Non Local Means filter to a real seismic dataset has proven to increase signal to noise ratio while preserving fault edges, however we found that different parameters were needed for different processing targets. As we have shown in chapter 4, using a neighborhood window value of 9 resolves the very deep reflections better, although it results in an "over-smoothed" appearance of seismic data in the shallower part. This particularly has to be avoided for NLM filtered data as an input for Sparse Spike Deconvolution, as using too large of search window and filter strength will smoothed out very small features, which might contributes to the high frequency content of the data which we want to be recovered after Sparse Spike Deconvolution.

The long computational time of NLM compared to other random noise filtering method such as f-x deconvolution and eigen vector filtering also makes it challenging, especially on 3D dataset. We found that using search window of 50 and neighborhood window of 9 are viable for 2D dataset, while for 3D dataset it can be very computationally expensive. This problem can be solved by parallelizing the code, which is very feasible as the algorithms scales very well with multiple computation cores. Several techniques were developed in the recent years to improve the computational efficiency of NLM, such as windowed application of partial data (Maraschini and Turton 2013), and uses of specific convolutional kernels and non-square search window and neighborhood window (De Gaetani et al. 2016), although those are outside the scope of this research.

Sparse Spike deconvolution with combined ℓ_1 norm and ℓ_2 norm regularization for maximum sparsity and smoothness constraints were found to increase vertical resolution and preserves reflection amplitudes and structures. The increased resolutions reveals new reflection packages and small geological features from the data. Applying Sparse Spike Deconvolution after NLM results in bandwidth enhanced data with better lateral continuity of the reflection and higher signal to noise ratio. However, due to depth dependency of time windowed smoothed wavelet extraction, different results can be produced from different choices of time window. We found that using a quite large time window between 2000 to 3500 ms targeting mid-depth to deep reflectors gives satisfying deconvolution result for both dataset with few noise artifacts.

4.2 Reprocessing approach for imaging geothermal reservoirs in the Netherlands

The reprocessed seismic data with just conventional processing shows to produce quite significant improvement over the old processed data. Our processing shows that Pre-Stack Kirchoff Time Migration algorithm used in our processing was better at imaging structures and faults than the post stack time migration used in the old data. The radon demultiple algorithm used also attenuates the multiples better on the marine

line, and the statics correction on the land line shows to produced more geologically realistic flat reflections on the shallow part of the land line. Overall, conventional processing with added Non Local Means Filter and Sparse Spike Deconvolution are proven to give better seismic images compared to the old images. The higher vertical resolution of Sparse Spike Deconvolution especially makes the previously non-visible small structures such as small faults, wedges, and channels emerge from seismic data. This is especially important for geothermal prospecting.

As we discussed in the first chapter, the challenges in seismic reflection for enhanced geothermal prospecting are weak reflection amplitudes resulting in a low signal to noise ratio and a low resolution in the deep section (Schmelzbach et al. 2016). Although NLM and Sparse Spike deconvolution were found to improve the signal to noise ratio and vertical resolution in the mid depth section of Rotliegend reservoir, the offset limitation factor still hampers their results on the imaging of deep section of Dinantian reservoir. Based on this fact, we suggest where necessary for new seismic acquisition with larger offset to get the maximum results on the Dinantian reservoir imaging.

4.3 Further Research and Improvement

Although seismic reflection images have vertically varied structures,amplitude, and noise level, they are more or less laterally uniform. This suggest that the usage of non-square spatially elongated search window and neighborhood window on NLM algorithm may improve the results. Also, as have been shown by De Gaetani et al (De Gaetani et al. 2016), the usage of a non-Gaussian kernel for similarity measurement can improve the results and performance of NLM. Further research regarding the kernel usage and NLM performance needs to be done. In Sparse Spike Deconvolution, a blind deconvolution approach (Chan and C.-K. Wong 1998) which solves the reflectivity and wavelet simultaneously during the inversion can prevent the wavelet uncertainty effects induced by our windowed wavelet estimation.

5 Conclusion

We have investigated a seismic processing scheme for imaging geothermal reservoirs which include high resolution sparse spike deconvolution and Non Local Means filtering after conventional seismic reprocessing work. Non Local Means filtering increases signal to noise ratio while preserving edges and small features like faults and fractures which are important for enhanced geothermal systems.

Our sparse spike deconvolution method of ℓ_1 norm regularization combined with ℓ_2 norm regularization smoothing constraints produced results with superior vertical resolution and enhanced frequency band-width. Moreover, it preserves reflection amplitudes and structures which is important for seismic interpretation.

Applying Non Local Means Filter before sparse deconvolution provides stronger reflection lateral continuity and coherency, and overall increasing signal to noise ratio of the bandwidth enhanced seismic data.

Evaluation of new processed seismic data with NLM and Sparse spike deconvolution applied with well data and previous interpretation gives us better delineation of Rotliegend reservoir Reservoirs while preserving small features like faults and edges from enhanced resolution higher signal to noise ratio. Limitations of the acquisition offsets however still remain on the very deep section of Dinantian Geothermal Reservoirs. To maximize geothermal exploration potential for ultra-deep reservoirs, we suggest where necessary re-acquisition combined with new unconventional processing techniques to give maximum results.

Bibliography

Acar, Robert and Curtis R Vogel (1994). "Analysis of bounded variation penalty methods for ill-posed problems". In: *Inverse problems* 10.6, p. 1217.

Bonar, David and Mauricio Sacchi (2012). "Denoising seismic data using the nonlocal means algorithm". In: *Geophysics* 77.1, A5–A8.

Bovik, Alan C (2010). *Handbook of image and video processing*. Academic press.

Buades, Antoni, Bartomeu Coll, and J-M Morel (2005). "A non-local algorithm for image denoising". In: *Computer Vision and Pattern Recognition, 2005. CVPR 2005. IEEE Computer Society Conference on*. Vol. 2. IEEE, pp. 60–65.

Canales, Luis L et al. (1984). "Random noise reduction". In: *1984 SEG Annual Meeting*. Society of Exploration Geophysicists.

Carpentier, S and P Steeghs (2016). "Final Report Work Package 7.1: New active seismic processing techniques developed". In: *EU Project IMAGE* 7.

Cetin, M. "Feature-enhanced synthetic aperture radar imaging', 2001". In: *PhD, College of Engineering, Boston University, Boston, MA*.

Cetin, Mujdat, William C Karl, and David A Castanón (2003). "Feature enhancement and ATR performance using nonquadratic optimization-based SAR imaging". In: *IEEE Transactions on Aerospace and Electronic Systems* 39.4, pp. 1375–1395.

Chan, Tony F and Chiu-Kwong Wong (1998). "Total variation blind deconvolution". In: *IEEE transactions on Image Processing* 7.3, pp. 370–375.

Chapman, NR and I Barrodale (1983). "Deconvolution of marine seismic data using the l 1 norm". In: *Geophysical Journal International* 72.1, pp. 93–100.

De Gaetani, CI et al. (2016). "Practical Aspects of Non Local Means Filtering of Seismic Data". In: *78th EAGE Conference and Exhibition 2016*.

Debeye, HWJ and P Van Riel (1990). "Lp-NORM DECONVOLUTION 1". In: *Geophysical Prospecting* 38.4, pp. 381–403.

Galbraith, Mike et al. (1991). "Random noise attenuation by fx prediction: A tutorial". In: *1991 SEG Annual Meeting*. Society of Exploration Geophysicists.

Geman, Donald and Chengda Yang (1995). "Nonlinear image recovery with half-quadratic regularization". In: *IEEE Transactions on Image Processing* 4.7, pp. 932–946.

He, Ran et al. (2014). "Half-quadratic-based iterative minimization for robust sparse representation". In: *IEEE transactions on pattern analysis and machine intelligence* 36.2, pp. 261–275.

Jaarsma, B et al. (2013). "Exploring Dinantian Carbonates in the SNS-New Data Offering New Insights". In: *75th EAGE Conference & Exhibition incorporating SPE EUROPEC 2013*.

Karslı, Hakan, Recep Güney, and Mustafa Senkaya (2017). "Post-stack high-resolution deconvolution using Cauchy norm regularization with FX filter weighting". In: *Arabian Journal of Geosciences* 10.24, p. 551.

Maraschini, Margherita and Neill Turton (2013). "Assessing the impact of a Non-Local-Means random noise attenuator on coherency". In: *SEG Technical Program Expanded Abstracts 2013*. Society of Exploration Geophysicists, pp. 4294–4298.

Milkereit, B and D Eaton (1998). "Imaging and interpreting the shallow crystalline crust". In: *Tectonophysics* 286.1-4, pp. 5–18.

Rudin, Leonid I, Stanley Osher, and Emad Fatemi (1992). "Nonlinear total variation based noise removal algorithms". In: *Physica D: nonlinear phenomena* 60.1-4, pp. 259–268.

Sacchi, Mauricio D, Danilo R Velis, and Alberto H Cominguez (1994). "Minimum entropy deconvolution with frequency-domain constraints". In: *Geophysics* 59.6, pp. 938–945.

Schmelzbach, Cédric et al. (2016). "Advanced seismic processing/imaging techniques and their potential for geothermal exploration". In: *Interpretation* 4.4, SR1–SR18.

Tarantola, Albert (2005). *Inverse problem theory and methods for model parameter estimation*. Vol. 89. siam.

Taylor, Howard L, Stephen C Banks, and John F McCoy (1979). "Deconvolution with the ℓ_1 norm". In: *Geophysics* 44.1, pp. 39–52.

Tikhonov, Andrei Nikolaevich (1963). "On the solution of ill-posed problems and the method of regularization". In: *Doklady Akademii Nauk*. Vol. 151. 3. Russian Academy of Sciences, pp. 501–504.

Trickett, Stewart et al. (2008). "F-xy Cadzow noise suppression". In: *2008 SEG Annual Meeting*. Society of Exploration Geophysicists.

Van Hulten, FFN (2012). "Devono-carboniferous carbonate platform systems of the Netherlands". In: *Geologica Belgica*.

Velis, Danilo R (2007). "Stochastic sparse-spike deconvolution". In: *Geophysics* 73.1, R1–R9.

Vogel, Curtis R and Mary E Oman (1998). "Fast, robust total variation-based reconstruction of noisy, blurred images". In: *IEEE transactions on image processing* 7.6, pp. 813–824.

Wang, Juefu and Mauricio Sacchi (2008). "Structure-and-Amplitude-Preserving Multi-Channel Deconvolution". In: *CSPG CSEG CWLS Convention, Canada*, pp. 729–732.

Wang, Juefu, Xishuo Wang, Mike Perz, et al. (2006). "Structure preserving regularization for sparse deconvolution". In: *2006 SEG Annual Meeting*. Society of Exploration Geophysicists.

Wang, Yang and Haomin Zhou (2006). "Total variation wavelet-based medical image denoising". In: *International Journal of Biomedical Imaging* 2006.

Wiest-Daesslé, Nicolas et al. (2007). "Non-local means variants for denoising of diffusion-weighted and diffusion tensor MRI". In: *International Conference on Medical Image Computing and Computer-Assisted Intervention*. Springer, pp. 344–351.

Wong, Theo Edward, Dick AJ Batjes, and Jan de Jager (2007). *Geology of the Netherlands*. Edita-the Publishing House of the Royal.

Yilmaz, Özdoğan (2001). *Seismic data analysis*. Vol. 1. Society of Exploration Geophysicists Tulsa.